Final Report

Integration of a Real-time Traffic State Estimation and a Decentralized Game-Theoretic Traffic Signal Controller

Amr Shafik
Virginia Tech Transportation Institute
Phone: (540) 231-1500; Email: ashafik@vt.edu

Hesham A. Rakha
Virginia Polytechnic Institute and State University
Charles E. Via, Jr. Department of Civil and Environmental Engineering
Virginia Tech Transportation Institute
Phone: (540) 231-1505; Fax: (540) 231-1555; Email: HRakha@vt.edu

Date
September 2025

Prepared for the Safety and Mobility Advancement Regional Transportation and Economics Research Center, Morgan State University, CBEIS 327, 1700 E. Coldspring Lane, Baltimore, MD 21251

ACKNOWLEDGMENT

This research was supported by the Safety and Mobility Advancement Regional Transportation and Economics Research Center at Morgan State University and the University Transportation Center(s) Program of the U.S. Department of Transportation.

Disclaimer

The contents of this report reflect the views of the authors, who are responsible for the facts and the accuracy of the information presented herein. This document is disseminated in the interest of information exchange. The report is funded, partially or entirely, under grant number 69A3552348303 from the U.S. Department of Transportation's University Transportation Centers Program. The U.S. Government assumes no liability for the contents or use thereof.

1. Report No. SM28	**2. Government Accession No.**	**3. Recipient's Catalog No.**
4. Title and Subtitle Integration of a Real-time Traffic State Estimation and a Decentralized Game-Theoretic Traffic Signal Controller		**5. Report Date** September 16, 2025
		6. Performing Organization Code
7. Author(s) *Include ORCID #* Amr Shafik (https://orcid.org/0000-0002-8689-9955) Hesham Rakha (https://orcid.org/0000-0002-5845-2929)		**8. Performing Organization Report No.**
9. Performing Organization Name and Address Virginia Tech Transportation Institute 3500 Transportation Research Plaza, Blacksburg, VA 24061		**10. Work Unit No.**
		11. Contract or Grant No. 69A3552348303
12. Sponsoring Agency Name and Address US Department of Transportation Office of the Secretary-Research UTC Program, RDT-30 1200 New Jersey Ave., SE Washington, DC 20590		**13. Type of Report and Period Covered** Final, September 2024 - August 2025
		14. Sponsoring Agency Code
15. Supplementary Notes		

16. Abstract

The report presents an integrated approach to adaptive traffic signal control by combining advanced traffic state estimation and adaptive optimization techniques. A two-stage adaptive Kalman filter (KF) algorithm is proposed to estimate turning movements and refine upstream density and queue sizes using probe vehicle data and detector measurements. Tested on data from Orlando, the method improves estimation accuracy significantly—reducing turning movement estimation error by up to 50% and queue size errors by 32.8%. The estimation algorithm is then integrated with a Decentralized Nash-Bargaining (DNB) traffic signal controller to optimize signal timings, even with incomplete vehicle trajectory data. Evaluations in Toronto and Orlando show that the DNB-KF system outperforms traditional traffic control strategies under limited data conditions. Additionally, the study explores two more optimization methods: the LDR cycle length adjustment and an enhanced DNB controller. Both methods use real-time traffic states to reduce delays and fuel consumption, achieving up to 37.7% delay reduction and 7.4% fuel savings. Overall, this research demonstrates that combining accurate traffic state estimation with adaptive, game-theoretic signal control leads to more efficient and sustainable urban traffic management, even with partial traffic data.

17. Key Words:		**18. Distribution Statement**	
19. Security Classif. (of this report): Unclassified	**20. Security Classif. (of this page)** Unclassified	**21. No. of Pages** 54	**22. Price**

Table of Contents

Abstract

Effective adaptive traffic signal control requires accurate traffic state estimation and adaptive optimization strategies to enhance urban mobility. This paper introduces a two-stage adaptive Kalman filter (KF) algorithm to estimate and predict critical traffic states, leveraging probe vehicle trajectory data and upstream detector measurements. The first stage estimates turning movement (TM) counts near signalized intersections, while the second stage refines upstream approach density and queue size estimations. Evaluation using drone-collected and simulated data from a four-legged intersection in Orlando, Florida, demonstrates that the proposed approach significantly enhances estimation accuracy, with TM estimation standard deviation reductions of up to 50% and queue size estimation improvements of up to 32.8% over the baseline. The method provides reliable traffic state predictions across varying market penetration levels, demonstrating its readiness for real-world implementation.

Building on this foundation, this research integrates the adaptive Kalman filtering algorithm with an advanced Decentralized Nash-Bargaining (DNB) traffic signal controller to address incomplete vehicle trajectory data. The joint DNB-KF controller utilizes estimated traffic states to optimize phase sequences and splits in scenarios with limited connected vehicle penetration. Performance evaluation at two signalized intersections in Toronto, Canada, and Orlando, Florida, indicates that the integrated system outperforms state-of-the-practice traffic control methods, including optimal pre-timed and actuated control. By demonstrating the controller's effectiveness in realistic conditions where full traffic information is not available, this study highlights the potential of advanced estimation techniques to improve adaptive traffic signal control.

Furthermore, the research evaluates two additional optimization strategies: the Laguna-Du-Rakha (LDR) cycle length optimization method and an enhanced DNB controller. These approaches optimize signal timing by dynamically adjusting control parameters based on real-time queue lengths and approach densities. Simulations at an isolated intersection in Toronto show that the optimized cycle length approach reduces delays by 25.6% and fuel consumption by 5.9%, while the DNB controller achieves a 37.7% reduction in delays and a 7.4% improvement in fuel efficiency.

By integrating accurate traffic state estimation with adaptive control strategies, this research contributes to the development of intelligent urban traffic management systems, enabling more

efficient mobility. The findings demonstrate that combining advanced estimation methods with game-theoretic and optimization-based traffic control enhances performance, even under incomplete traffic information, making these approaches well-suited for future connected and automated vehicle environments.

Introduction

Effective traffic signal control (TSC) is essential for optimizing urban mobility and minimizing congestion at signalized intersections. Traditional TSC strategies are typically classified into three main types: fixed timing, actuated, and adaptive control (Papageorgiou et al., 2003). Fixed-time signal plans are derived offline based on historical traffic flow and turning movement (TM) data, aiming to minimize vehicle delays and maximize intersection capacity utilization. Methods such as Webster's equation (Webster & Cobbe, 1958) and the Laguna-Du-Rakha (LDR) formula (Calle-Laguna et al., 2019) have been developed to optimize cycle length calculations. However, these methods rely on static assumptions and lack real-time adaptability.

Real-time adaptive traffic signal control requires accurate estimation and prediction of key traffic state variables, including turning movements and queue sizes, which are critical for dynamic signal timing optimization (Blokpoel & Vreeswijk, 2016). Traditional methods for obtaining these data—such as manual counts and fixed-point sensors like loop detectors and video cameras—are labor-intensive, costly, and subject to accuracy limitations due to environmental factors [Papageorgiou et al., 2003]. Recent advancements in connected vehicle (CV) technologies provide an opportunity to enhance traffic state estimation using probe vehicle data, including vehicle positions, speeds, and headings (Blokpoel & Vreeswijk, 2016). While CV data offers real-time availability and high granularity, its effectiveness is constrained by market penetration rates (Abdelghaffar & Rakha, 2021). At low penetration levels, relying solely on probe vehicle data can lead to unreliable estimates, necessitating robust estimation techniques (Blokpoel & Vreeswijk, 2016).

To address these challenges, this study integrates an adaptive Kalman filtering (KF) algorithm with a Decentralized Nash-Bargaining (DNB) traffic signal controller to enhance real-time traffic state estimation and adaptive control. The proposed two-stage estimation approach first estimates TMs based on probe vehicle trajectories and upstream detector data rates (Abdelghaffar & Rakha, 2021). The second stage refines queue size and approach density estimates, providing essential traffic state information for real-time signal optimization. Unlike previous Kalman filter applications, which often focused on highway traffic and relied on historical data for covariance error calculations, this approach is specifically designed for signalized intersections and adapts in real time (Blokpoel & Vreeswijk, 2016).

The integration of the KF-based traffic state estimation with the DNB controller enables signal timing adjustments even under incomplete trajectory data conditions, improving the adaptability of traffic signal control strategies. The effectiveness of this joint DNB-KF system is evaluated at two signalized intersections—one in Toronto, Canada, and another in Orlando, Florida—across varying market penetration levels. Additionally, the study compares the performance of the enhanced DNB controller and an optimized cycle length method to state-of-the-practice approaches, such as pre-timed and actuated control.

By leveraging advanced estimation techniques and game-theoretic traffic control, this research contributes to the development of intelligent urban traffic management systems. The findings demonstrate that integrating real-time Kalman filter-based traffic state estimation with adaptive signal control can enhance mobility, and reduce congestion, even in scenarios with incomplete traffic information (Blokpoel & Vreeswijk, 2016).

Literature Review

Traffic State Estimation Using Kalman filters

Estimation of Turning Movement Counts

Numerous efforts in the existing literature have approached the turning movement estimation problem at signalized intersections using loop detector data. As the approaching traffic flow counts are relatively easy to obtain using detectors or other stationary sensors, multiple methods have been proposed to infer TMs using approaching flows. The manual trial-and-error technique is one of the methods that requires obtaining inflow and outflow traffic at all approaches of the intersection. This approach is considered tedious and difficult in terms of mathematical calculations and efficiency (Schaefer, 1988). Some studies presented more robust techniques to estimate the most likely origin-destination matrix for intersections, which best replicates the observed approach counts, such as the work of (Hauer et al., 1981), which estimated the matrix using a likelihood maximization approach using Kruithof's algorithm. This technique showed acceptable estimation accuracy; however, prior knowledge about actual TMs is critical for performing this approach. In addition, this method requires the deployment of detectors in all directions that carry traffic to and from the intersection. (Van Aerde et al., 2003) developed a tool for estimating an origin-destination (OD) demand matrix. The tool utilizes a maximum-likelihood-based numerical solution that does not require flow continuity at the network nodes. It is noted that the origin-destination problem is under-specified, where multiple solutions will provide a match to the counts. The maximum likelihood is used to select the most likely solution out of these. A seed matrix can also be used to bias the solution towards the seed matrix.

More recent studies presented other methods to estimate TMs, such as the work of (Xu et al., 2013), which developed an automatic TM identification system (ATMIS) that estimates TMs on a real-time basis. Another study by (X. Zhang et al., 2012) estimated TMs using a nonlinear programming approach using inflow and outflow counts. This approach shows high consistency compared to actual TMs. However, these methods still require outflow detectors to obtain acceptable estimates.

(A. Chen et al., 2012) also used a nonlinear path flow-based algorithm to estimate TMs at the network level based on counts across the entire network. The study showed promising results in

terms of estimation accuracy. However, the algorithm's iterative process is considered difficult for real-time field applications in which TM estimations are required for short periods (e.g., 10-30 s).

Some studies used a genetic algorithm for TM estimations, such as the work of (Jiao et al., 2005), which estimated TMs in real-time by minimizing the deviations between observed and estimated traffic counts. Ghanim et al. (Ghanim & Shaaban, 2019) used artificial neural networks (ANNs) for the estimation. Results of the developed ANN model showed that ANNs can be used to accurately estimate TMs. (Mousavizadeh et al., 2021) utilized probe vehicle data for turning rate estimation at large-scale urban networks using a wavelet transform decomposition, using an estimation model that requires historic TM data. However, training machine learning models and training such estimation models based on historical data are considered computationally expensive and cannot be generalized beyond the context of the training data, such as applications to different characteristics of intersections, driving behavior, and demand patterns.

Some studies adopted a nonlinear least-square approach for the TM estimation problem such as the work of (Lan & Davis, 1999), which performed real-time TM estimation using partial counts on urban networks. The study employed a recursive nonlinear least-square approach using a partial set of detector counts. Similarly, (Mirchandani et al., 2001) presented a least-square minimization TM prediction algorithm implemented on a real-time basis. The algorithm is based on phase-to-phase counts that require the current turning proportions for prediction.

Finally, recent advancements in CV technologies have also been leveraged to estimate TMs, such as the work of (Saldivar-Carranza et al., 2021), which used CV trajectory data to estimate TMs at signalized intersections. Entry and exit trajectory headings were used to detect the number of movement clusters using k-means clustering, which were assigned to a TM. A matching accuracy of up to 98% was achieved for over 1.1 million analyzed trajectories.

Queue Size Estimation from Probe Vehicles

The real-time queuing information at isolated intersections is essential information for the optimal control of traffic signals. Advancements in connected and automated vehicle technology allow the traffic signal controller to use probe vehicle data to make queue size estimates. There are vast contributions in the literature on the topic of queue estimation, which is mainly addressed in two

primary estimation techniques as follows: the input-output method (Cao et al., 2014) and the shockwave theory. The input-output method estimates the number of vehicles within the queue, whereas the shockwave theory emphasizes the spatial extent of the queue. Furthermore, the queue estimation timeframe setting is categorized into a cycle-by-cycle queue length estimation and the real-time queue estimation (Wei et al., 2022).

Various methods of real-time queue estimation are reported in the literature, such as the work of (Comert & Cetin, 2011), which used a statistical method to estimate queue size in real-time from probe vehicle data. Based on the position of the probe vehicles in the queue, the queue size is estimated by a derived analytical expression. The study showed high estimation accuracy. However, it assumed that the marginal probability of queue size distribution is known, which is prior knowledge that is unavailable in many cases. (Liu et al., 2019) used a Markov model to estimate real-time queue size utilizing probe vehicle data. The average traffic flow rate, historical queue size data, and the stopping states for arriving probe vehicle data were used in the estimation procedure. The estimation scheme was tested for multiple market penetration levels of CVs. Results indicated high estimation accuracy and efficiency in handling the randomness in the system. One drawback is that the study relied on historical data, which might not be readily available. In addition, the categorization of queue size estimation by TM was also overlooked.

Another study by (Zhao et al., 2019) proposed a series of novel methods for real-time queue size estimation from probe vehicles. The proposed methods exploited the stopping positions of probe vehicles. The traffic volume and total queue size for each movement were obtained using the aggregated historical trajectory data. Study limitations include the inaccurate estimation of the market penetration rate using the last stopping position of probe vehicles. (Rostami-Shahrbabaki et al., 2020) used a data fusion approach to estimate the second-by-second queue length. The proposed method showed notable estimation accuracy and efficiency.

(Wei et al., 2022) adopted an empirical Bayes method to estimate the cycle-based queue length, which showed significant estimation performance. (Hao et al., 2014) used a Bayesian network model for estimating cycle-by-cycle queue length. The study reported that 5% is the minimum market penetration rate for the practical application of queue estimation using probe vehicles. However, the cycle-to-cycle queue estimation methods are only considered applicable to

conventional traffic signal controllers where the phase lengths are known. This is unlike other adaptive signals where the phase length is not known in advance.

Traffic State Estimation Using Kalman Filters

Kalman filters have been widely used in various traffic management and control applications. For instance, Kalman filters have been employed to estimate vehicle density and space-mean speeds on highways (Aljamal et al., 2019; van Lint & Djukic, 2012). These studies demonstrated that Kalman filters could provide reliable state estimates, but their primary focus was on highway traffic, where traffic dynamics are more predictable compared to urban traffic networks. As a result, their applicability to signalized intersections remains limited.

(Antoniou et al., 2007) applied a nonlinear Kalman filter algorithm to calibrate online dynamic traffic assignment models. The proposed method achieved high accuracy and computational efficiency. However, the study mainly focused on large-scale traffic networks and did not address traffic state estimation at the microscopic level, such as signalized intersections, which require more granular and dynamic estimation methods.

(Emami et al., 2019) utilized a Kalman filter algorithm for short-term traffic flow prediction in a connected vehicle (CV) environment, while the study demonstrated the effectiveness of incorporating CV data into prediction models, it assumes a high market penetration rate of connected vehicles. This assumption may not be held in real-world scenarios with lower CV adoption rates, limiting the method's practical applicability.

(Bekiaris-Liberis et al., 2016) used a Kalman filter to estimate mixed traffic density on highways using the average speed of connected vehicles. This method showed high estimation accuracy but relied heavily on connected vehicle data, making it less effective for low CV penetration levels. Additionally, the study focused on highway traffic conditions, where traffic flow is more homogeneous compared to urban settings.

Kalman filters have also been applied to turning movement estimation at signalized intersections such as the work of (Jiao et al., 2014), which proposed a Bayesian approach combining a back-propagation neural network and a revised Kalman filter. This method achieved high estimation accuracy by leveraging both historical and real-time data. However, the reliance on historical data

can be a significant limitation in situations where such data are scarce or unavailable, and the computational complexity of the method may hinder real-time applications.

(X. Zhang et al., 2012) employed a Kalman filter technique based on an extended cell transmission model (ECTM) to estimate TMs for adaptive traffic signal control systems, while the method provided reliable traffic state estimates, its accuracy decreased during highly dynamic traffic conditions, such as sudden fluctuations in demand, which are common at signalized intersections.

(Enjedani & Khanal, 2023) developed a Kalman filter TM estimator using probe vehicle data. The study showed improved estimation accuracy by considering probe data representative of total traffic flow at low CV penetration levels. However, the method's reliance on historical data limits its applicability to short-term TM estimation and real-time traffic signal optimization.

(S. Hu et al., 2022) applied an Extended Kalman Filter (EKF) for queue estimation at signalized intersections, integrating a machine learning-based shockwave queue propagation model. The study demonstrated accurate real-time queue estimates. However, EKF's accuracy is highly dependent on the quality of the machine learning model training, which can be challenging due to the extensive historical data requirement.

Adaptive Kalman Filtering

Previous Kalman filtering applications are based on prior knowledge of the error parameters in the filter, which are the measurement noise covariance matrix, as well as the process noise covariance matrix Q. Most of the previous work utilized historical data to estimate fixed error matrices, assuming that the error ranges will remain constant. This assumption might not always be true, in addition, historical data may not be available in many applications. As such, the concept of adaptive Kalman filtering emerged, where prior knowledge of the noise matrices Q and R are not required.

An adaptive Kalman filtering method was first proposed by Mehra in 1970 (Mehra, 1970), where the author developed a technique to obtain unbiased estimates and consistent estimates of R and Q for discrete systems. This technique is considered useful in cases where the noise matrices are unknown. The proposed technique is also extended to continuous filtering systems with high filtering efficiency. (Brown & Rutan, 1985) also proposed a method to obtain the unknown measurement error matrix R from an empirically chosen window. The study showed significant

accuracy improvement in the estimated parameters. Another study by (Karasalo & Hu, 2011) also proposed a procedure to estimate the noise matrix Q. The study used system models $x = f(s)$, $y = h(x) + v$ to recover the observation $h(x)$ without prior knowledge of the system dynamics.

Adaptive filtering has also been used for many applications in vehicle tracking and traffic state estimation. For example, Hu et al., 2003 applied an adaptive Kalman filter algorithm to GPS data for vehicle navigation (C. Hu et al., 2009). The study showed the efficiency of the adaptive algorithm in capturing sudden changes in the vehicle's motion as well as accounting for measurement errors. Some studies have explored adaptive filtering approaches for traffic state estimation on highways. For instance, (X. Chen et al., 2019) used an adaptive rolling smoothing (ARS) method to estimate the traffic flow rate, speed, and time occupancy to mitigate traffic congestion dynamics. The ARS method adjusts filter parameters in a rolling horizon, making it suitable for online applications by dynamically estimating measurement noise from real-time data. However, this method is primarily designed for highways and does not account for the unique challenges of traffic state estimation at signalized intersections.

Similarly, (Wang et al., 2008, 2009) employed adaptive extended Kalman filters to estimate traffic states on highways, while these methods effectively addressed traffic congestion dynamics on freeway segments, they overlooked traffic state estimation at urban intersections, where traffic flow patterns are more complex due to the presence of traffic signals, queuing dynamics, and turning movements.

To summarize, the use of Kalman filtering has been extensively studied in traffic state, turning movement, density, and queue estimation. However, most existing studies focus on overall traffic state estimation without differentiating by turning movement, which is critical for adaptive traffic signal controllers that rely on movement-specific data. Additionally, the majority of traffic state estimation methods have been applied on highways, where traffic flow is more predictable, while fewer efforts address the more complex and dynamic conditions at intersection approaches. Many methods incorporate historical traffic data within Kalman filters to account for estimation errors, but these data are often unavailable or unreliable in real-world applications. The reliance on machine learning models alongside Kalman filters further limits practical applicability, as these methods depend heavily on the availability of training data and cannot generalize beyond the scope

of the historical data used. Furthermore, some studies assume high connected vehicle (CV) penetration rates, which is unrealistic in many traffic systems and introduces additional computational complexity that may hinder real-time implementation. Finally, most existing approaches fail to provide real-time updates at short intervals, making them less effective for adaptive traffic signal control in rapidly changing traffic conditions. Addressing these shortcomings is crucial to developing more accurate, movement-specific, and practical traffic state estimation methods for real-time traffic management at intersections.

Traffic Signal Control

Contemporary traffic signal control (TSC) strategies are classified into three types: fixed timing, adaptive, and actuated traffic control (Papageorgiou et al., 2003). The fixed time TSC is derived offline based on the knowledge of the historical traffic flow and turning movements for each of the intersection approaches. The signal plan optimization goal is to minimize the average vehicle delay and maximize the intersection capacity utilization. A phasing scheme is designed so that the optimization goal is achieved, where each phase is given a split according to its relative flow-to-saturation flow ratio compared to other phases. The optimal cycle length is obtained from a nonlinear total delay function such as that derived by Webster and Cobbe (Webster & Cobbe, 1958) and (Calle-Laguna et al., 2019) which proved that Webster's equation over-estimates the cycle length and provides an optimum cycle length calculation formula (LDR formula) that overperforms Webster's formula.

On the other hand, fixed-time TSC is considered insensitive to the dynamic nature of traffic flow which can fluctuate significantly in short periods of time. As such, adaptive TSC is introduced to reevaluate traffic conditions and optimize the signal plan at each phase using the current traffic, which is obtained using traffic sensors such as traffic cameras or inductive loop detectors (Mirchandani et al., 2001). In addition, the actuated TSC is also used to mitigate the effect of the traffic stochasticity on the optimum signal plan using vehicle actuation (Papageorgiou et al., 2003). Furthermore, there are other TSC strategies such as the use of neural networks for real-time optimization of TSC (Srinivasan et al., 2006), and the implementation of reinforcement learning within adaptive TSC (El-Tantawy et al., 2014).

Recent research efforts utilized the concepts of game theory for the traffic signal optimization problem. The problem is perceived as a game of multiple rational participators who coordinate interactively and cooperate to achieve the maximum benefit, with each player's decisions representing rational individual behavior. Game theory is considered an important tool in many fields, such as communications, economics, business, politics, psychology, and evolutionary biology. In the transportation field, game theory has been used in areas like route choice modeling, traffic management, logistics, transportation systems analysis, and traffic control (Ahmad et al., 2023; Ahmad & Al-Fagih, 2024; Linglong et al., 2010; Raghothama & Meijer, 2014; H. Zhang et al., 2010).

Research efforts have applied game theory to traffic management, such as Bazzan's work utilizing evolutionary game theory techniques for traffic signal coordination (Bazzan, 2005). Alvarez and Poznyak also applied game theory to the traffic control problem. The method was applied to an isolated intersection, where a Nash-Bargaining controller outperformed adaptive TSC in terms of queue length minimization (Alvarez & Poznyak, 2010). (Linglong et al., 2010) have also shown that the game theoretic TSC algorithm improved the control performance compared to the fixed time TSC.

Abdelghafar and Rakha (Abdelghaffar & Rakha, 2019, 2021; Elouni et al., 2021) developed a decentralized Nash-Bargaining TSC that provides a flexible phasing scheme as well as phasing splits that adapt to the changing demand levels. Each signal phase is considered as a game player, where all players cooperate to maximize their benefits. A significant performance improvement is reported of up to 64% reduction in vehicle delay. On the other hand, the study overlooked the intergreen time at each phase switch, which resulted in overestimated benefits. The study also overlooked the lost time per phase, leading to a more frequent switching pattern without taking the lost time at each switch into consideration.

Methodology

Traffic State Estimation and Prediction

System Overview

A Kalman filter is an efficient recursive minimum variance estimator that follows a prediction-correction scheme. The Kalman filter integrates the recent previous state estimate with the current state observation to perform state estimation and future state projections. This algorithm was first developed by Kalman in 1960 (Kalman, 1960). The filter uses previous state estimates, new state observations, and projections of previous states to generate refined estimates of the current state variables. This is done by separating the random noise inherent in the observations and fusion with projections of previous states. Kalman filters are used in numerous industrial applications such as object tracking, signal processing, and navigation (Auger et al., 2013), which makes it suitable for time series applications to estimate TMs on a real-time basis.

In this study, a Kalman filter algorithm was employed in a two-stage approach to estimate and predict TMs in the first stage and density and queue size in the second stage.

The Kalman filter algorithm is utilized within a two-stage approach. At the first stage, it is utilized for TM estimation, while at the second stage, it is utilized for density and queue size estimation.

As depicted in Figure 1 the algorithm follows a multi-stage process for estimation and prediction, where the system makes state predictions in one stage and then the state is updated using observed data in another stage. In this system, historical data are not required to calibrate the error matrices, but the current observations and the perceived market penetration rate are used to quantify the process and observation noise matrices.

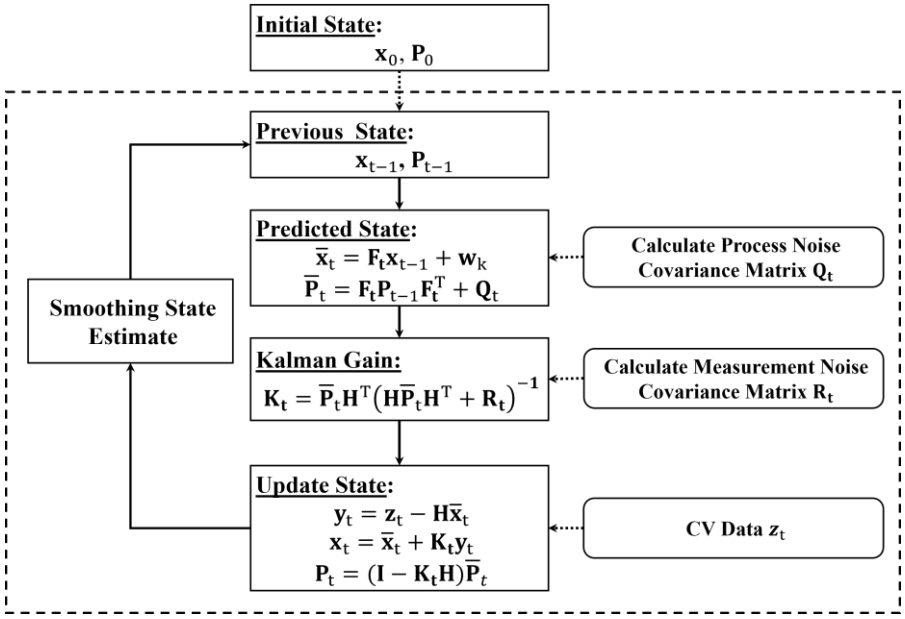

Figure 1: Kalman filter process

Figure 1 shows the general estimation and prediction framework that utilizes the observed measurements from probe vehicles and stationary detectors to estimate the traffic state parameters. First, the market penetration rate is estimated in real-time. Then, the first-stage Kalman filter estimates and predicts the turning movement rates for the current and the next time steps, respectively. Second, the predicted turning rates are used to estimate and predict the queue length and the traffic density in the second stage of the Kalman filtering process.

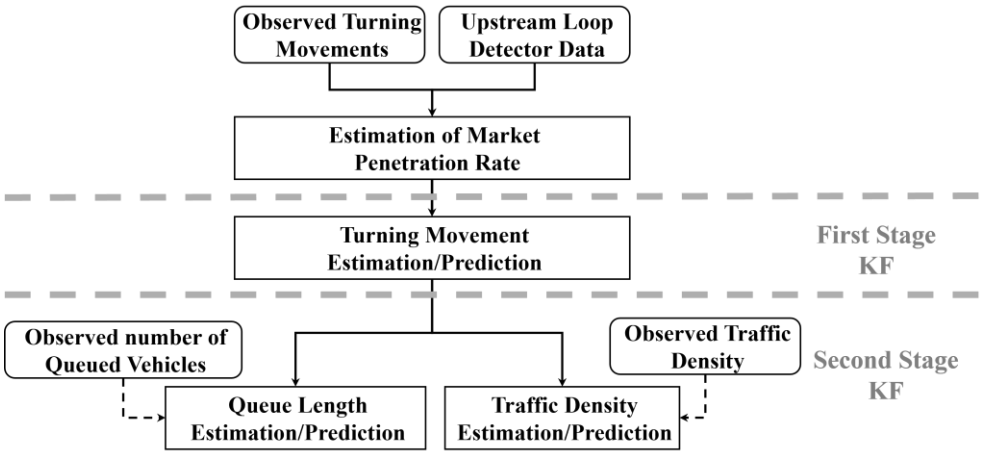

Figure 2: General process overview

As shown in Figure 1, the Kalman filter uses the previous traffic state estimates to obtain the predicted state using the process matrix F . The prediction function incorporates the time-varying process noise covariance matrix Q . The process matrix F represents the rate of change in loop detector readings, calculated using current and previous loop detector data. This rate is assumed to be constant for a single prediction step, which is reasonable for short prediction periods of 10-30 seconds.

The Kalman gain K is calculated using the updated state covariance matrix and the time-varying measurement noise covariance matrix. In the update step, the estimated state variable and covariance matrix are calculated upon receiving probe vehicle observations. Finally, exponential smoothing is applied to enhance the filter's performance. Subsequent sections provide more elaboration on these steps.

State Variables

In this study, because the objective is to estimate TMs at intersection approaches in the first stage, the state variables are defined by the traffic flow rate (in veh/hr.), turning right (x_{rt}), heading through (x_{thr}), and turning left (x_{lt}), respectively. The state vector x; ($n \times 1$), where n is the number of state variables, is defined as follows:

$$\mathbf{x} = \begin{bmatrix} x_{rt} & x_{thr} & x_{lt} \end{bmatrix}^{\mathsf{T}}$$

These TM state variables can be observed from the combination of probe vehicle trajectory data and stationary detector data, where the probe CV vehicles broadcast TMs, which represent samples of the total flows. The Kalman filter approach employs a rollback method to determine probe vehicle headings. This means the system goes back in time until it locates at least one vehicle for each TM. If no probe vehicles are observed turning in a particular direction, the system considers the TM as zero. These observations are then balanced by the total approaching traffic flow obtained from the upstream loop detector. The accuracy of the TM observations relies on the current level of market penetration in each experiment, while the detectors capture the approaching volumes.

In the second stage, a single variate Kalman filter is applied for each direction to estimate and predict the traffic density (in veh/km) on the upstream link as well as the number of queued vehicles per movement (in vehicles for the left and through movements). Upstream locations and

speeds of probe vehicles are used as measurements for the estimation of the current upstream density and queues.

Prediction Step: State Transition Function

In this step, the current state vector is projected to the short-term future as a process model. Kalman filters future projections of one step ahead in the future, typically referred to as a prediction using the current and past state observations.

The state transition function, as shown in the equation below, utilizes the process matrix F_t, the current state x , and the state transition noise w_k to provide the next state vector, which represents the predicted state vector of the next time step. It is noted that the state transition function F_t is time-varying based on the current and previous loop detector observations. The transition function is shown as follows:

$$\bar{\mathbf{x}}_\mathbf{t} = \mathbf{F}_\mathbf{t}\mathbf{x}_\mathbf{t} + w_k$$

where w_k; $(n \times 1)$; $N(0, Q_t)$ denotes the state transition (process) noise with dimensions $(n \times 1)$, following a normal distribution with mean 0 and process noise matrix Q_t.

The state covariance matrix $\overline{P_t}$ is calculated in this step using the current covariance matrix $\mathbf{P_t}$, the process matrix F_t, and the process noise covariance matrix $\mathbf{Q_t}$. The state covariance update is represented in the equation below as follows:

$$\bar{\mathbf{P}}_\mathbf{t} = \mathbf{F}_\mathbf{t}\mathbf{P}_\mathbf{t}\mathbf{F}_\mathbf{t}^\mathsf{T} + \mathbf{Q}_\mathbf{t}$$

The process noise matrix $\mathbf{Q_t}$ will be explored in the next subsection.

Process Noise Covariance Matrix

In the context of this problem, the time-varying process noise covariance matrix $\mathbf{Q_t}$; $(n \times 1)$ is defined as the matrix composed of the prediction error variance of each of the state variables. $\mathbf{Q_t}$ is recalculated at each iteration in each of the filter stages to account for the prediction error.

The process noise in the first stage Kalman filter represents the prediction errors caused by the assumption that the growth factor is identical for all turning movements. Since the actual growth factor will not be the same for all turning movements, the error should be quantified using the

observed growth factor for each individual turning movement obtained from CVs, As well as the market penetration level. As such, the standard error formula, shown below, quantifies how the observed individual growth rates vary from the actual individual growth rates for the population. Subsequently, the matrix $\mathbf{Q_t}$ is comprised of the standard error for each turning movement on the matrix diagonal.

$$Standard\ Error\ (S.E.) = Z\sqrt{\sigma_p^2/n} = Z\sqrt{p \times (1-p)/n}$$

In the second stage, since the density and queue size predictions are based on the estimated TMs in the first stage, the covariance matrix P_t, which represents the confidence in TM estimates, is used to calculate the prediction covariance matrix, resulting in an adaptive Kalman filter.

The Process Model: Stage 1

The process model $\mathbf{F_t}$ is derived at each Kalman filtering stage based on the dynamic nature of the state variable. The process model for the first stage filter is provided below, where the process matrix $\mathbf{F_t}$ is a diagonal matrix comprised of the growth factor $\mathbf{GF_t}$ over short intervals using the traffic flow continuity (conservation of the number of vehicles). In this stage, the process model $\mathbf{F_t}$ is based on the growth factors ($\mathbf{GF_t}$) estimated using loop detector measurements, as shown below. The most recent observed flow growth rate is assumed to remain constant, which is a reasonable assumption over small time intervals.

$$\mathbf{F}_t = diag(GF_t, GF_t, GF_t)$$

$$\frac{\partial k(x,t)}{\partial t} + \frac{\partial q(x,t)}{\partial x} = 0$$

where x denotes the spatial coordinate in the traffic flow direction, k is the traffic stream density, q is the traffic flow, and t is the time instant.

$$GF_t = L_t / L_{t-\Delta t}$$

where L_t represents the traffic flow measured upstream via loop detectors or other stationary sensors.

The Process Model: Stage2

In the second stage, the input-output queue estimation method (Cao et al., 2014) is used to predict the number of queued vehicles as well as the traffic density. The turning movements, obtained from the first-stage Kalman filter, are used to determine the arrival flows. The traffic signal indication for each movement on each approach is also used to determine the departure rate. The traffic density process model employed a method similar to the queue estimation process model. The equation below utilizes the input-output model to calculate the predicted vehicle queue (or the traffic density).

$$u_{t+\Delta t} = \begin{cases} u_t + q_{\text{in}} \times \Delta t - q_{\text{out}} \times (\Delta t - t_{\text{lost}}), & \text{for green phases.} \\ u_t + q_{\text{in}} \times \Delta t - q_{\text{out}} \times t_{\text{eg}}, & \text{for red phases.} \end{cases}$$

where u_t is the current vehicle queue or the traffic density, q_{in} is the average traffic flow obtained from the first stage KF, and q_{out} is the average discharge rate.

Update Step: Measurement Function

The Kalman filter refines the projected state using probe vehicle observations represented by the measurement vector z_t. As shown below, the residual vector y_t is calculated using the predicted state vector $\overline{x_t}$ and the measurement vector z_t. Because the Kalman filter computes the residual vector in the measurement space, the matrix **H** is used for the transition. In the second stage Kalman filter, probe vehicles are used to measure the number of stopped vehicles in the queue. It is noted that the matrix **H** is omitted in the second stage Kalman filter because the density and queue size estimation problem is univariate, where the matrix **H** equals [1].

$$\mathbf{y}_t = \mathbf{z}_t - \mathbf{H}\bar{\mathbf{x}}_\mathbf{t}$$

Where z_t is the measurement vector and **H**; $(m \times n)$ is the state-to-measurement transition matrix, defined as follows:

$$\mathbf{H} = \begin{bmatrix} 1 & 0 & 0 \\ 0 & 1 & 0 \\ 0 & 0 & 1 \\ 1 & 1 & 1 \end{bmatrix}$$

Measurement Noise Matrix

The Kalman filter employs the measurement noise covariance matrix $\mathbf{R_t}$; $(n \times n)$ to capture the inherent uncertainty in the measurement vector. This matrix quantifies the variance of expected errors in these measurements, which is based on the level of market penetration of the probe vehicle data. The calculation procedure of the $\mathbf{R_t}$ matrix is based on the sampling error approach, where the matrix is calculated at each KF update iteration using the measured number of vehicles and the detector data representing the total number of vehicles.

The error variance is derived from the sampling error, which quantifies how much confidence we can place on the observed number of TMs. Subsequently, the Kalman gain $\mathbf{K_t}$ is calculated using the equation below and used to update the state estimate x and the state covariance matrix $\mathbf{P_t}$, as shown below. The variable x is considered a recursive solution of the optimal state estimation problem, which means that the system state can be estimated solely based on the previous state estimate and the new observation y_t. This property of the approach is computationally efficient and makes it suitable for real-time applications (van Lint & Djukic, 2012).

$$\mathbf{K_t} = \bar{\mathbf{P}}_\mathbf{t}\mathbf{H}^\mathsf{T}(\mathbf{H}\bar{\mathbf{P}}_\mathbf{t}\mathbf{H}^\mathsf{T} + \mathbf{R}_t)^{-1}$$
$$\mathbf{x_t} = \bar{\mathbf{x}}_\mathbf{t} + \mathbf{K_t}\mathbf{y_t}$$
$$\mathbf{P_t} = (\mathbf{I} - \mathbf{K_t}\mathbf{H})\bar{\mathbf{P}}_\mathbf{t}$$

The Observation Model: Stage 1

The observation model z_t is derived at each Kalman filtering stage based on the dynamic nature of the state variable. In the first stage, the observation model is given in the equation below, where the turning movement measurement represents the flow rate of probe vehicles within a dynamic rollback window, factored by the market penetration rate. This window is selected dynamically so

that at least one connected vehicle is observed at each turning movement, assuming that probe vehicles are present at all turning movements.

$$\mathbf{z}_t = \frac{[N_{\text{thr,t}}, N_{\text{rt,t}}, N_{\text{lt,t}}, N_{\text{tot},t}]^T}{MP_t}$$

where N_d represents the flow rate of probe vehicles for direction d. MP_t represents the market penetration proportion at time t.

The Observation Model: Stage 2

In the second stage, the positions and speeds of the probe vehicles are used to infer the number of queued vehicles, and the traffic density within the measurement region. The inferred market penetration rate is used to estimate the total number of vehicles. The equation below shows the observation model for the second stage; there, the measurement vector depends on the vehicle longitudinal position on the link (x) at each turning movement at time t, as well as the market penetration rate.

$$\mathbf{z}_t = g[x_{v,dir,t}, MP_t]$$

Estimate Smoothing

The probe vehicle observations are subject to sudden changes or outliers, which can significantly impact the performance of the Kalman filter's recursive process. As such, an exponential smoothing technique is applied to the Kalman-filtered state estimates to further reduce the noise and enhance their accuracy and precision. The equation below shows the exponential smoothing formula, in which the value α variables are tuned according to the level of market penetration.

The α values close to zero put more weight on past values, making the forecast smoother and slower to react to recent changes. This is used to limit fluctuations in the traffic state estimates due to the high errors at low market penetration levels, while higher values close to 1.0 put more weight to observations at higher confidence cases. In this study, α values vary linearly from 0.4 to 1.0 linearly based on the value of market penetration level, where the value 0.4 corresponds to the minimum MPL and 1.0 corresponds to MPL = 100. The minimum value of α (0.4) is calculated

using the trial-and-error method by testing different values of α and selecting the one that minimizes the forecast error.

$$\tilde{\mathbf{x}}_t = \alpha \mathbf{x}_t + (1-\alpha)\tilde{\mathbf{x}}_{t-\Delta t}$$

Traffic Signal Optimization using Decentralized Nash Bargaining

Nash-Bargaining Algorithm

The Nash-Bargaining addresses the traffic signal optimization problem as a multi-player game where each signal phase represents a rational player in the game. All the players coordinate and cooperate to make an optimal decision agreed upon by all parties. Each mutually agreeable decision involves a payoff or a penalty for the players.

In this problem, decisions determine which phases receive a green light other phases receive a red light. The game strategy is defined as maximizing expected total payoff among all players when giving a green light to a particular phase. In this process, each applicable scenario is evaluated, and the benefits or penalties are calculated for all players, resulting in a total payoff for all available decisions.

The Threat Point

The threat point (i.e., disagreement point) is defined as the point that each player avoids reaching irrespective of the decision being made. As such, each of the available decision options must satisfy this condition. As such, this represents a benchmark for the minimum benefits that each player is willing to achieve. In this problem, the threat point is represented as the maximum number of vehicles that can be stored in lane groups at each signal phase before they begin spilling into other lanes or upstream links, which creates congestion. The threat point is calculated as follows:

$$d_j = \sum_{i=1}^{I} L_i \times k_{jam}$$

where the threat point is represented by d_j, which is calculated using the storage length of all the lanes that carry traffic that corresponds to the phase j, L_i is the length of the lane *i*, and k_{jam} is the jam lane density.

Payoff Evaluation

The process of payoff evaluation determines the payoff and penalties corresponding to each player at each available decision prior to decision-making. The payoff evaluation is based on the utility function U_i. The player utility is computed for each player based on the queue length or the

approach density, where the number of vehicles corresponding to a phase leverages the utility value of this phase. The payoff value U_i is calculated as shown in the equation shown below.

$$U_i = \prod_{j=1}^{J} d_j - u_{i,j}$$

where the total utility value of the decision scenario *i* is the multiplication of the difference between the queue capacity and the utility corresponding to that phase. $u_{i,j}$ is the utility value of each player *j* at each decision i.

Table 1: The Game Decision Scenarios and Payoffs

Scenario	Phases				Payoff
	1	**2**	**3**	**4**	
Scenario 1	Green	Red	Red	Red	U_1
	$u_{1,1}$	$u_{1,2}$	$u_{1,3}$	$u_{1,4}$	
Scenario 2	Red	Green	Red	Red	U_2
	$u_{2,1}$	$u_{2,2}$	$u_{2,3}$	$u_{2,4}$	
Scenario 3	Red	Red	Green	Red	U_3
	$u_{3,1}$	$u_{3,2}$	$u_{3,3}$	$u_{3,4}$	
Scenario 4	Red	Red	Red	Green	U_4
	$u_{4,1}$	$u_{4,2}$	$u_{4,3}$	$u_{4,4}$	

The game decision is based on the highest payoff value U_i, where the problem is constrained to prevent each player's utility from reaching the threat point. The problem formulation can be written as shown below:

$$\begin{aligned} &\max \quad U_i \\ &s.t. \quad u_{i,j} \in S, \quad u_{i,j} \leq d_j \end{aligned}$$

where the set *S* represents the utility space.

Queue and Density Prediction

In this research, the payoff utility function is calculated using two approaches: vehicle queues and approach density. In order to obtain information about the current utility value (i.e. queue length or density), it is assumed that the full vehicle information is available by either full vehicle connectivity with the infrastructure (V2I), or by using traffic cameras directed at each of the intersection approaches. As such, the number of vehicles ahead of the threat point is known. Furthermore, to estimate the payoff of each potential decision, upstream loop detector data is used to estimate the vehicle arrivals during the next DNB evaluation period. As such, the payoff of each decision in the game-theoretic framework can be estimated.

It is noted that using the queue length in the utility function only accounts for stopped vehicles (with stopping speed less than 4.5 km/hr.) as leverage for each approach during the payoff evaluation. This approach neglects other existing vehicles on the approach that travel at low speeds or are decelerating to a stop. In the other case, using approach density accounts for all vehicles in the approach regardless of their current speed at the time of payoff evaluation.

Solution Procedure

In this paper, two evaluation criteria are considered in the payoff calculation process as measures of performance (MOP): queue length and upstream traffic density. The system assumes either full vehicle connectivity to the DNB controller or the presence of traffic cameras at the intersection approaches, ensuring vehicle count information is available. At each step, the predicted utility value is calculated at the end of the DNB evaluation period for each player. Subsequently, the payoff values are calculated, and the optimal decision is made. The traffic signal then begins the inter-green period (yellow and all-red intervals) before switching to the selected green phase.

It is noted that the start loss at each phase switch is considered in the calculations for switching scenarios. Similarly, the end gain is also accounted for in the calculations. This approach prevents the system from recommending more frequent switches, which would lead to increased total lost time. Algorithm 1 illustrates the DNB solution procedure, which is performed each evaluation period.

Algorithm 1 The DNB Algorithm.

Input: $u_{0,j}$: the current utility value at time t_0 for phase j,
Δt: DNB evaluation period for the next phase.
Output: The optimal phase number.
for each scenario i **do**
  for each phase j **do**
    Initialize total phase utility $u_{i,j} = 0$
    for each lane group k in phase j **do**
      Calculate lane group utility $u_{i,j,k}$ at $t_0 + \Delta t$.
      Update total phase utility $u_{i,j} += u_{i,j,k}$
    end for
    Calculate total phase utility $u_{i,j}$ at $t_0 + \Delta t$.
  end for
  Calculate total scenario payoff $U_i = \prod_j d_j - u_{i,j}$ at $t_0 +$
  Δt.
end for
Determine the optimal scenario with the highest payoff U_i.
Implement the optimal scenario.

Traffic Signal Optimization using Incomplete Probe Data

The DNB traffic signal controller delivers optimal performance under ideal conditions with full real-time data on traffic density and queues, achievable either through complete vehicle connectivity or intersection detection cameras. However, since current connected vehicle adoption remains limited, such conditions are uncommon, making the system's theoretical performance an optimistic upper bound. To ensure practical applicability, the DNB controller is tested across varying market penetration levels, assessing its effectiveness under partial or imperfect data conditions.

To compensate for data gaps, the DNB algorithm employs the Kalman filter algorithm in this analysis, which estimates real-time traffic states (e.g., density, queues) by combining partial observations with system dynamics. The filter's outputs support the DNB system in two key ways:

1. Queue Estimation: The Kalman filter provides real-time queue lengths at each evaluation point, derived from detected stopped vehicles within the control region.
2. Density Prediction: For phase-length optimization, the filter predicts traffic density under different signal phasing scenarios, using inputs from the DNB controller.

This iterative process ensures the DNB system operates reliably even with incomplete data, refining its decisions at each control cycle.

Experimental Design

Data Collection

The evaluation of the proposed system involved a comprehensive analysis of real-world trajectory data sourced from a drone-based dataset. The detailed contextual information about the studied intersections is provided in the original publication by (Zheng et al., 2023). The dataset, which was specifically designed for urban traffic studies, focuses on the traffic dynamics at a four-legged signalized intersection situated at the intersection of Alafaya Trail and University Boulevard in Orlando, Florida. This location, illustrated in Figure 3, serves as a case study for assessing the effectiveness of the two-stage approach for TM and queue size estimations. The choice of this dataset is particularly significant, as it provides a realistic and dynamic representation of urban traffic scenarios, offering insights into the algorithm's performance under real-world conditions of actual traffic patterns and oscillations. In addition, using this dataset ensures that the evaluation process is performed in applicable scenarios, enhancing the credibility of the proposed system's performance assessment.

Figure 3: Four-legged signalized intersection at Alafaya Trail and University Boulevard in Orlando, Florida

Upstream Detector and CV Data

The raw trajectory data are transformed to mimic real-time probe vehicle data and upstream loop detector information, where traffic flow features like individual vehicle trajectories are extracted.

The total flow count on each approach is computed using the raw trajectory data. In addition, based on the market penetration level in each experiment, randomly sampled trajectories are selected to represent probe vehicles that their broadcast headings upon entering the intersection zone. The real-time information, including detector data and probe vehicle data, is fed to the two-stage approach. The evaluation utilized one hour of trajectory data collected at a frequency of 30 frames per second. Table 2 shows the total hourly demand for each approach per direction according to the data.

Table 2: Intersection demand rate in vehicles/hr. according to the drone-based vehicle trajectories

Approach	LT	THR	RT
NB	71	721	88
SB	188	806	100
EB	121	1223	134
WB	86	844	278

DNB Control Algorithm Evaluation

In order to evaluate the performance of the proposed DNB algorithm, the algorithm is applied at a four-legged intersection in downtown Toronto, Canada (the intersection of Front St. and Bay St.) illustrated in Figure 4. As shown in the figure, the intersection demand at the PM peak hour is shown for the year 2005, which represents the worst-case scenario at this intersection (El-Tantawy et al., 2014). The intersection features four approaches, each with an exclusive left turn pocket lane. Figure 5 shows the intersection phasing scheme considered in this study.

The intersection is a modeled microscopic simulation software environment developed in-house using Python that features characteristics of traffic flow, such as the Fadhloun-Rakha car-following model, Van-Aerde traffic stream model, vehicle dynamics model, and VT-CPFM-I fuel consumption model (Fadhloun & Rakha, 2020; H. Rakha et al., 2004, 2004; H. A. Rakha et al., 2011; Van Aerde & Rakha, 1995). The simulation model is calibrated so that the baseline results are consistent with the observed conditions and the base model as reported by El-Tantawy et al. (El-Tantawy et al., 2014). Furthermore, the demand input is modeled based on exponentially distributed arrivals, which reflects the random nature of vehicle arrivals. As such, the model can simulate the variability and randomness in traffic demand.

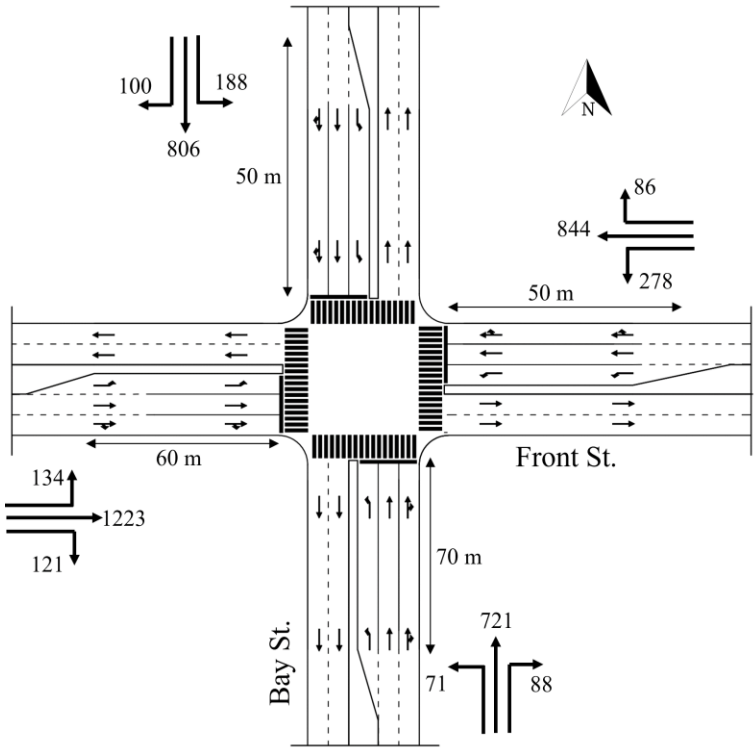

Figure 4: Intersection Layout and Demand in Vehicles/hour (Front St. and Bay St., Toronto

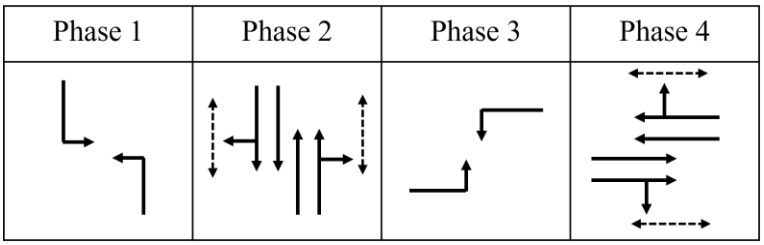

Figure 5: Toronto Intersection Phasing Diagram

Benchmarks

The proposed DNB algorithm is compared with the results of the optimal fixed-time TSC. In this paper, two methods are used to determine the optimal cycle length: Webster's method (Webster, 1958) and the LDR method (Calle-Laguna et al., 2019). The saturation flow rate is set at 1900 vehicles per hour per lane, the speed limit is 40 km/hr, and the yellow time is calculated as 3 seconds. Using these parameters, Webster's cycle length is calculated as 120 seconds with phase splits of (16, 34, 21, 49), and LDR's cycle length is calculated as 82 seconds with phase splits of (11, 23, 15, 33). Baseline intersection performance measures, such as vehicle delay, queue length,

and fuel consumption, are calculated for the two fixed-time plans and compared with the results of the proposed algorithm.

Results and Analysis

TM Estimation and Prediction Results

The TM estimation algorithm was evaluated for multiple cases with prediction horizons of 1, 5, and 10 s. In addition, several experiments were performed considering various levels of market penetration of probe vehicles ranging from 5% to 100%. Figures 6-8 show the algorithm performance in estimating TMs on the east-bound (EB) intersection approach at a market penetration level of 5%, 10%, and 20%, respectively. Each figure shows the hourly moving average number of turning vehicles for one hour for each of the following three TMs: through, right, and left. The plots show the distribution of actual TMs compared to the estimated number of TM counts as well as the probe vehicles. The figures below illustrate the TM estimation error compared to the filtered estimates, highlighting the efficiency of the proposed Kalman filter algorithm, where the estimated TMs have significantly less noise than those estimated by CV data, even at low levels of market penetration.

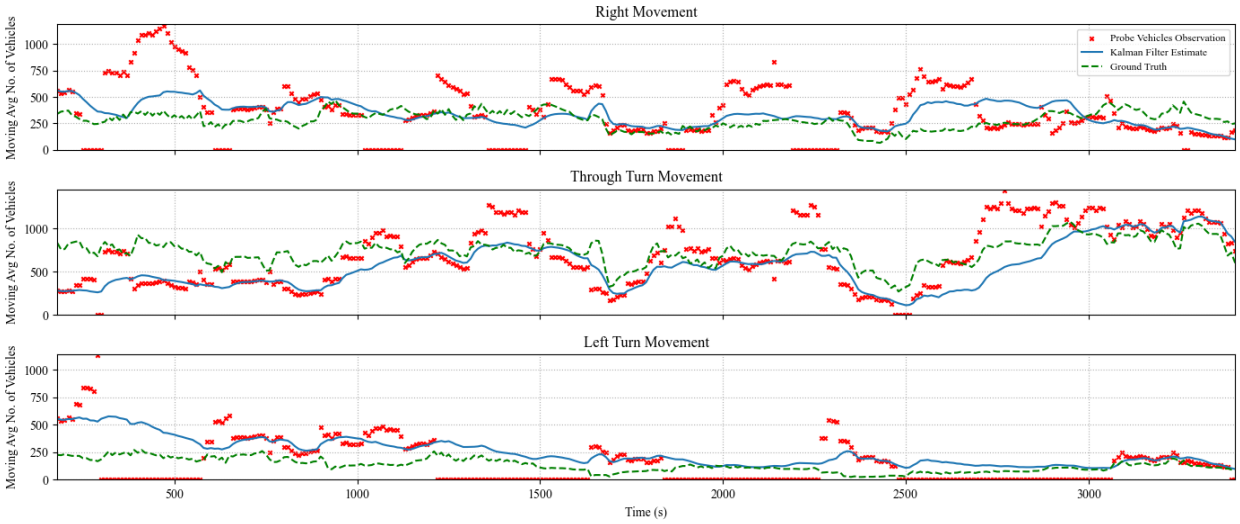

Figure 6: Comparison between Kalman filter-derived TM counts versus CV observations and ground truth counts for the EB approach at a MPL of 5%

Figure 7: Comparison between Kalman filter-derived TM counts versus CV observations and ground truth counts for the EB approach at market penetration = 10%

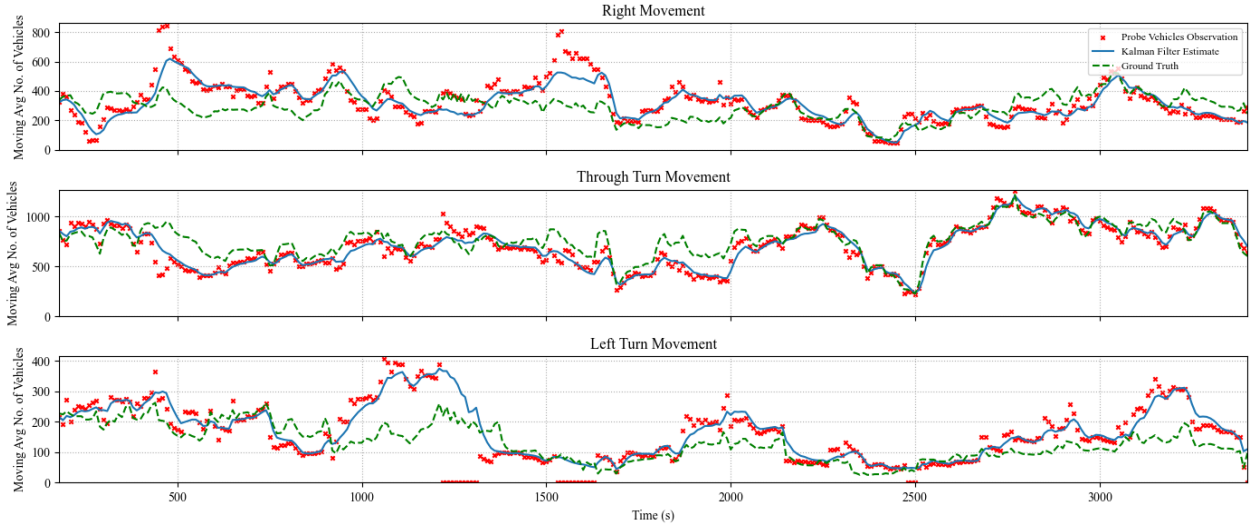

Figure 8: Comparison between Kalman filter-derived TM counts versus CV observations and ground truth counts for the EB approach at market penetration = 20%

Accuracy of Estimation and Prediction

To further assess the estimation errors of the proposed algorithm, Table 3 provides a comparison of the standard deviations (SD) associated with TM estimates derived from both the probe data and Kalman filtering approaches for market penetration levels of 5%, 10%, and 20%. Notably, the Kalman filtering approach demonstrates a significant enhancement in the SD of current real-time TM estimates. For instance, at a market penetration level of 5%, the proposed Kalman filter approach reduced the SD by 48%. Additionally, the SD of the Kalman filtering predictions is 92.8

vehicles/hr, further showcasing the accuracy of the Kalman filter in predicting TMs even at low levels of market penetration.

The findings were also evaluated by the results of the analysis depicted in Figure 9. For instance, at the 5% penetration level, the coefficient of determination R^2 advanced from -0.14 for probe-vehicle-estimated TMs to a significantly improved 0.70 for Kalman filter-estimated TMs at a market penetration level of 5%. Moreover, the Kalman filter predictions exhibit a coefficient of determination of 0.68, which is a substantial enhancement over the accuracy achieved when using only probe vehicle data. These results illustrate the effectiveness of the Kalman filter approach in refining TM estimates and providing reliable TM estimates that are representative of real-time traffic dynamics.

Table 3: A comparison between the SD of TMs (vehicles/hr.) derived from probe vehicle data and using Kalman filtering

Approach	Market Penetration Levels		
	5%	10%	20%
SD of probe vehicle-estimated TMs	174.1	138.8	56.1
SD of Kalman filter-estimated TMs	90.5	69.1	35.9
Estimation improvement	48.0%	50.1%	36.0%
SD of Kalman filter-predicted TMs	92.8	72.5	42.7

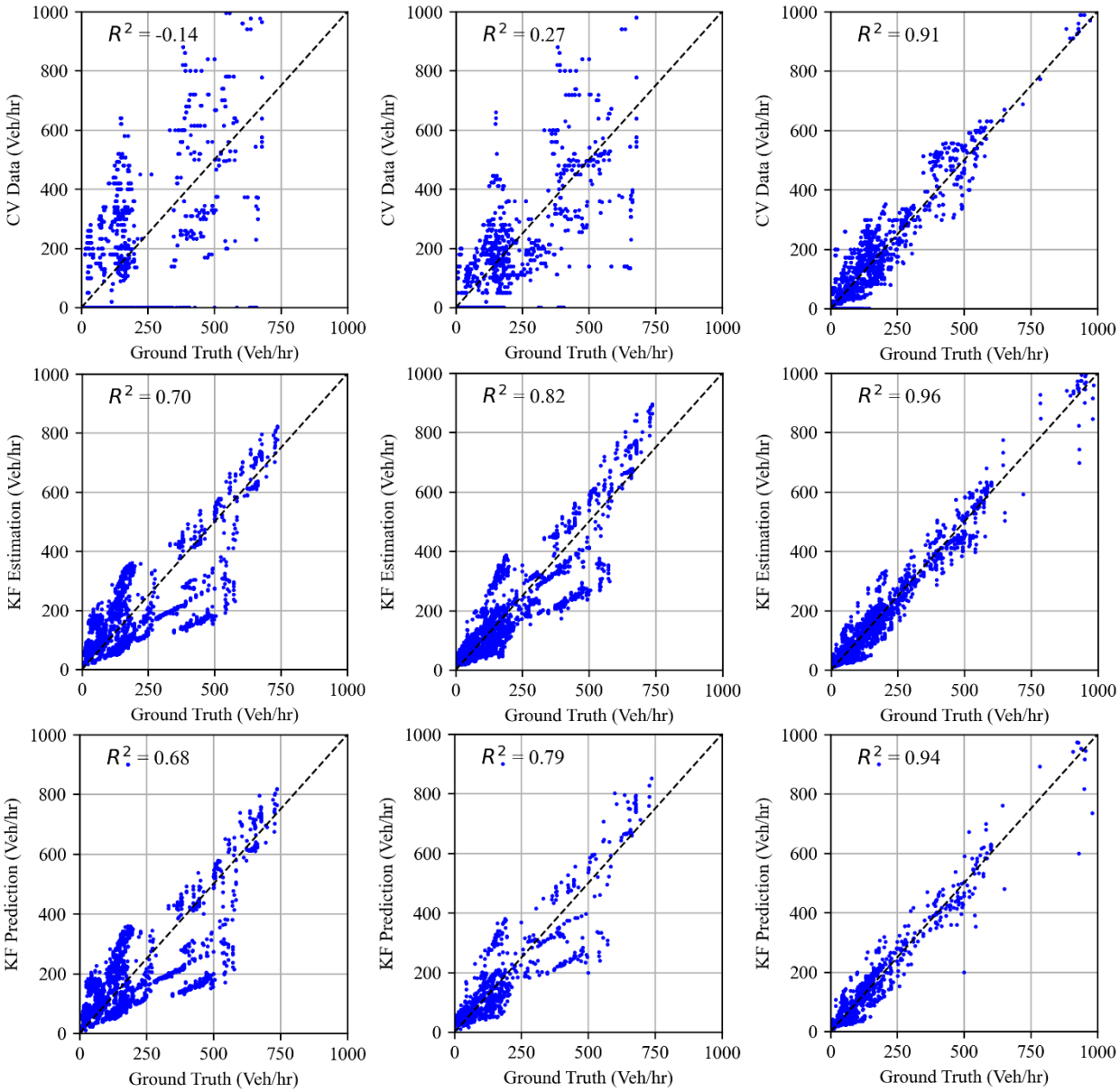

Figure 9: Correspondence between TM estimates and ground truth. (a) Market penetration = 5%; (b) market penetration = 10%; (c) market penetration = 20%

Figure 10 shows the probability distribution of the difference between the ground truth approach flows and the corresponding estimates/predictions generated by the Kalman filter algorithm. Notably, the deviations observed in TM estimates derived from probe vehicle data are significantly reduced. Furthermore, Figure 11 shows the root-mean-squared error (RMSE) values across various levels of CV market penetration implemented in this study. The outcomes reveal that the Kalman filter algorithm consistently outperforms solely CV-derived estimates in capturing the current system state. Furthermore, even at low CV market penetration levels, the Kalman filter algorithm

demonstrates improved predictive capabilities for TM counts, with an RMSE value ranging from 164 to 27 vehicles/hr at various MP levels, as shown in Figure 12, where the level of error is significantly lower than the estimated TM by probe vehicle data alone. This underlines the reliability of the proposed Kalman filter approach, which qualifies this algorithm to be used as a tool to provide TM counts for queue size estimation algorithms, as performed in this research. The algorithm also qualifies to be integrated with real-time traffic analysis and signal control systems, with varying degrees of CV market penetration levels.

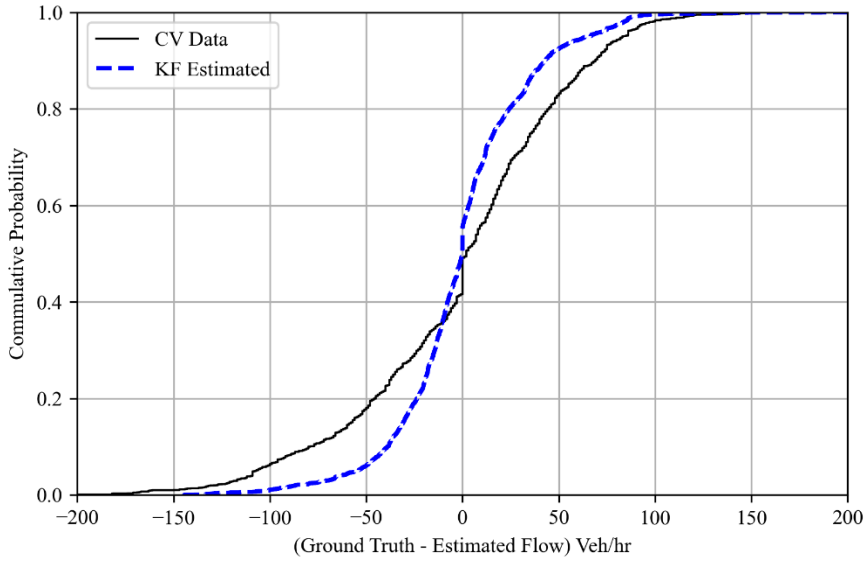

Figure 10: The cumulative probability of the difference between the ground truth and Kalman filter-derived estimated flows

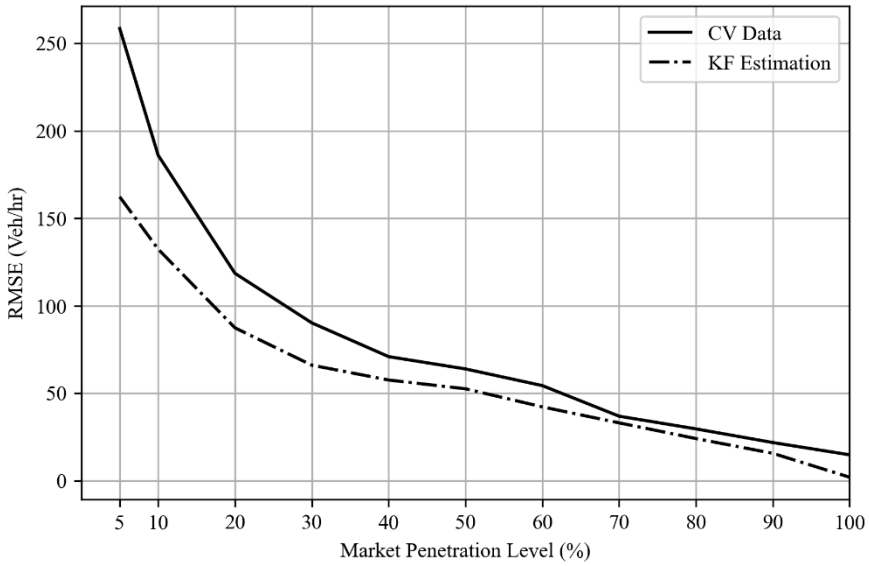

Figure 11: TM estimation accuracy results for different levels of market penetration

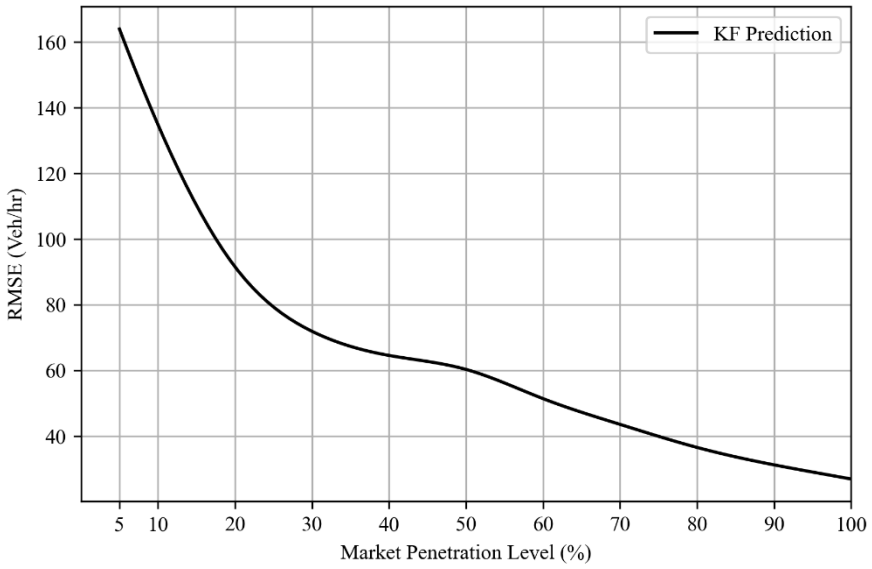

Figure 12: TM prediction RMSE results for different levels of market penetration.

Queue Size and Density Estimation Results

In this subsection, the second stage of the proposed approach is evaluated. The Kalman filter method was used for queue size and density estimation and compared with the baseline estimates using solely probe vehicle data. The TM estimates conducted at the first stage were utilized to estimate and predict the real-time queue size and density. The two-stage approach was implemented for the isolated signalized intersection for multiple levels of probe vehicle penetration ranging from 5% to 100% for each prediction horizon of 5 and 10 seconds. Figure 13 shows the queue size estimation results for the through and left TMs at the north-bound (NB) approach of the intersection for market penetration levels of 5%, 10%, and 20%, respectively.

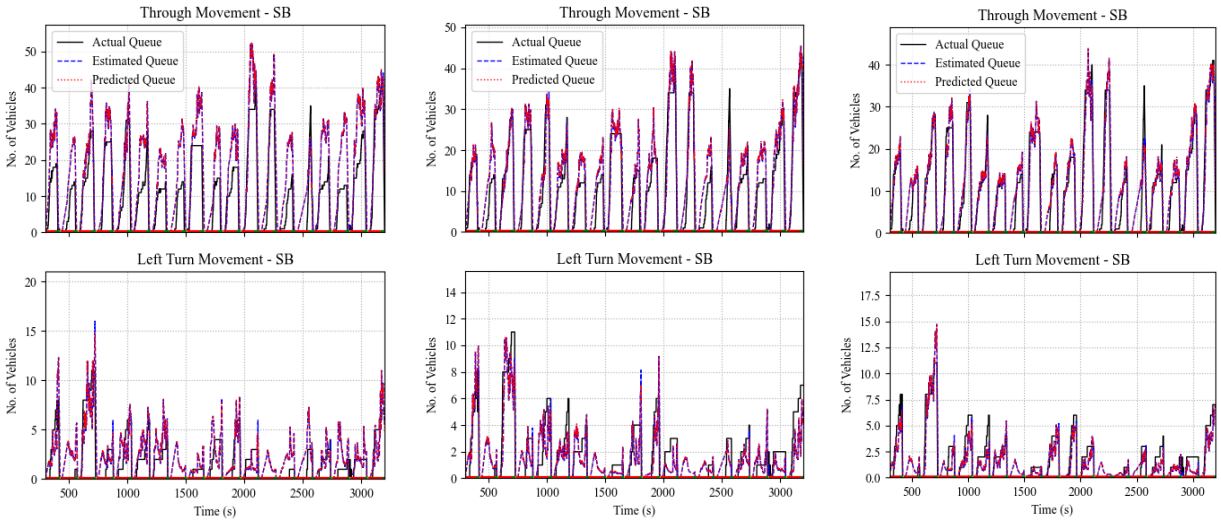

Figure 13: Comparison between queue estimation using the Kalman filter method and ground truth. (a) Market penetration = 5%; (b) market penetration = 10%; (c) market penetration = 20%.

Figure 14 illustrates the performance evaluation results of queue estimation and prediction. It is shown that the use of Kalman filtering for queue size estimation outperforms the baseline estimates using the probe vehicle data by up to 32.8%, which highlights the filter's capability to reduce the estimation noise at low levels of market penetration. However, at high levels of market penetration, the results show an insignificant impact from using Kalman filters compared to the sole use of probe vehicle data to derive queue size estimates. The figure also shows the prediction quantification results, where the level of error is consistent with the state estimation error results across various MP levels.

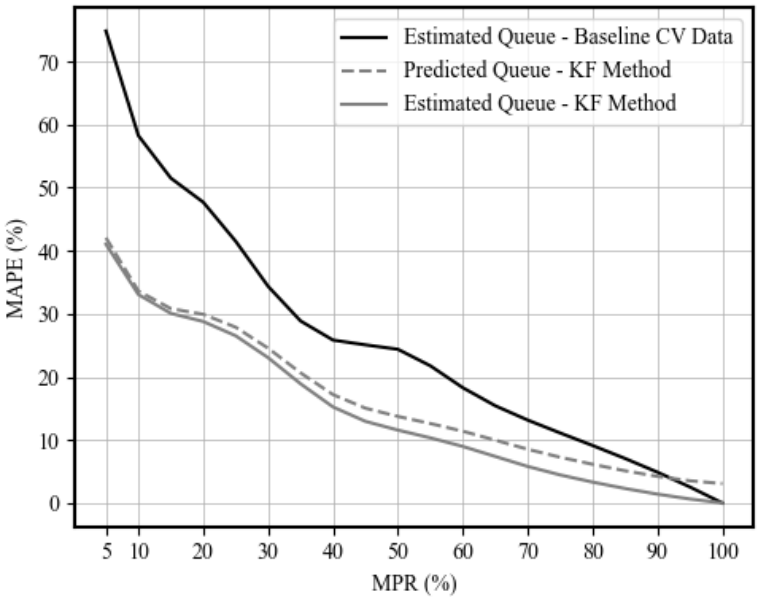

Figure 14: Queue estimation and prediction MOP results at different levels of market penetration.

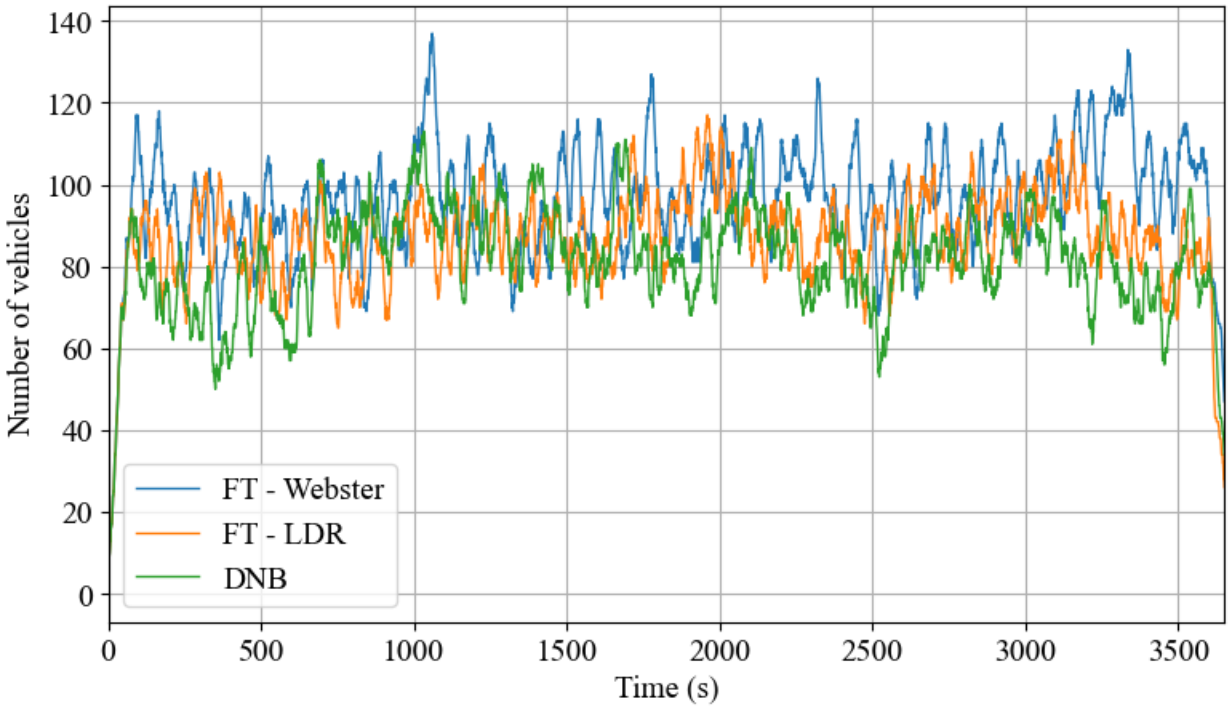

To quantify the estimation of upstream traffic density, Figure 15 shows the RMSE of the traffic density estimates (the density of vehicles traveling at upstream links in veh/km) and predictions using Kalman filters compared to the baseline method. Figure 15 shows improved estimation at various market penetration levels, where the RMSE improved by up to 21%. Figure 15 also shows the prediction performance of the filter, whose prediction accuracy is consistent with the estimation accuracy.

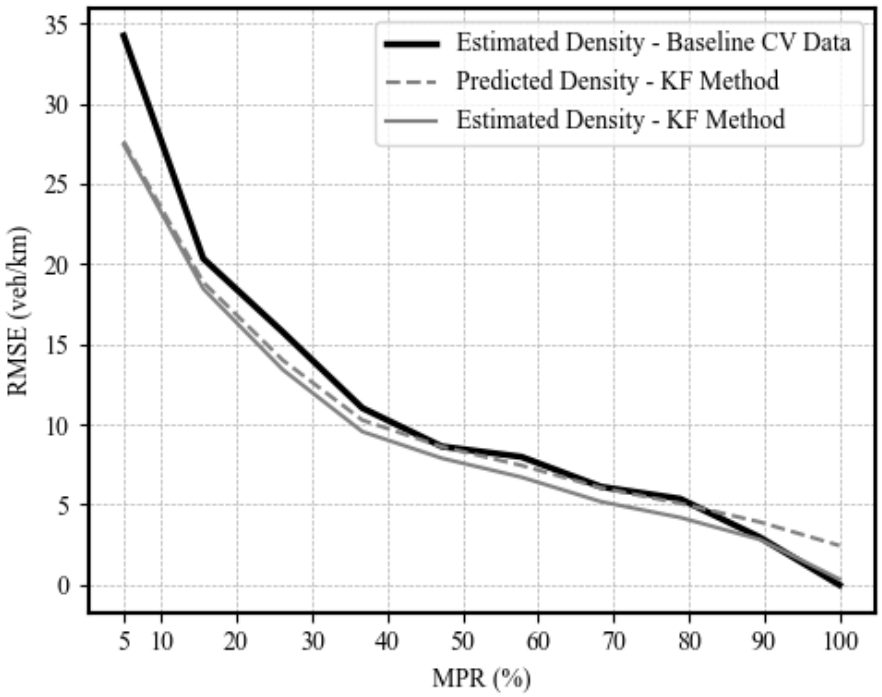

Figure 15: Density estimation and prediction RMSE results at different levels of market penetration.

Results of DNB Algorithm

This section presents the simulation results of the proposed DNB TSC algorithm. Several measures are extracted and compared with the optimal fixed-time plans. The next subsections present the detailed results and analysis of the system performance.

Number of Vehicles in the System

Figure 16 illustrates the number of vehicles in the system throughout the entire simulation period. This figure provides a visual representation of how the total number of vehicles in the system fluctuates with each implemented TSC plan. In this comparison, Webster's fixed-time plan results in the highest number of vehicles present in the system. This suggests that Webster's fixed-time plan may not be the most efficient in terms of minimizing congestion and managing traffic flow. The LDR fixed-time plan also results in a relatively high number of vehicles, although not as many as Webster's plan. On the other hand, the DNB controller generally results in a lower number of vehicles in the system throughout the simulation period. This indicates that the DNB controller is more effective in optimizing traffic flow and reducing congestion compared to the fixed-time plans. The lower vehicle count associated with the DNB controller suggests that it may be better suited for dynamic traffic conditions, providing more responsive adjustments to traffic signal timings based on real-time traffic data.

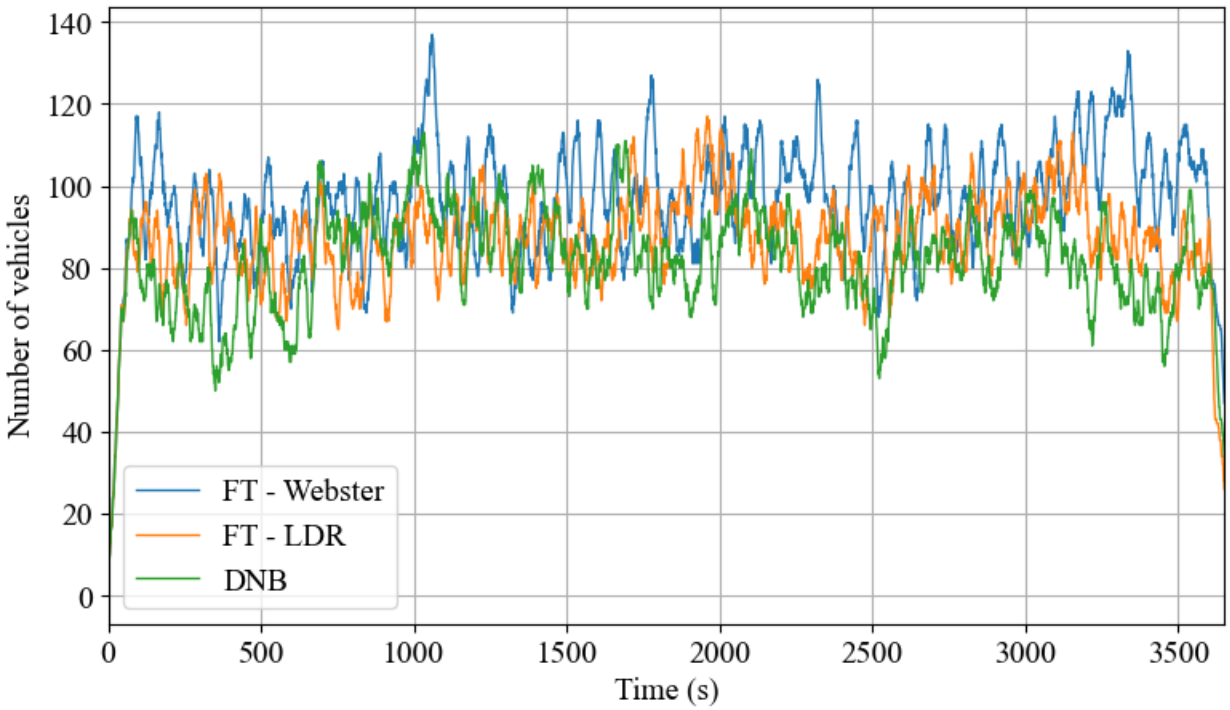

Figure 16: Number of vehicles in Simulation

Average Queue Length

Figure 17 presents the average queue length for three scenarios: Webster's fixed-time plan, the LDR fixed-time plan, and the DNB controller. It is shown that the DNB controller generally results in significantly lower average queues across most intersection approaches. Additionally, the LDR fixed-time plan demonstrates better performance compared to Webster's fixed-time plan, showing shorter queue lengths on average. It is noted that the LDR fixed-time plan achieves lower average queues than the DNB controller at certain left turns, such as WBL and SBL. This, in specific instances, can be attributed to the LDR fixed-time plan's optimization of green time, particularly for U-turns, effectively clearing queues more efficiently in these scenarios. However, the DNB controller results in lower average queues across the entire intersection.

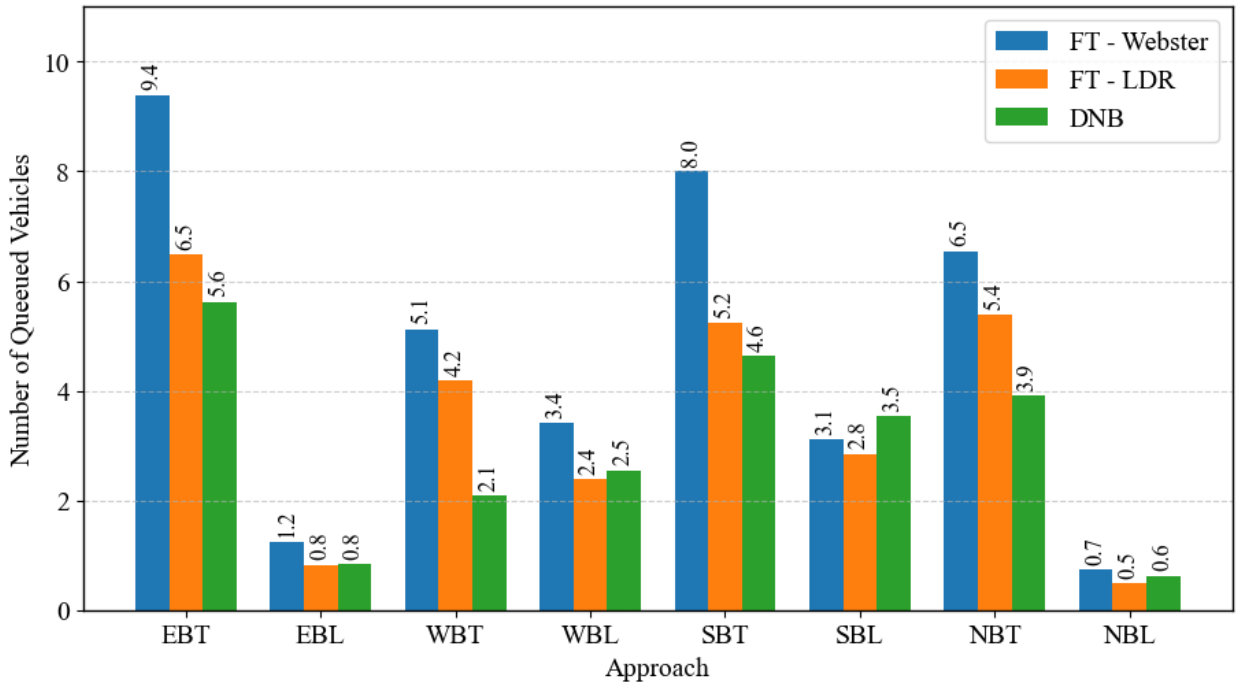

Figure 17: Average Queue Length at each Direction

Average Delay

Table 4 presents the average delay results for each of the signal control strategies. The table shows that the DNB controller significantly outperformed both Webster's and LDR's fixed-time plans in terms of reducing average delay. Specifically, the DNB controller achieved a delay reduction of up to 37.7% compared to Webster's fixed-time plan, indicating a significant improvement in signal control efficiency. The LDR fixed-time plan also demonstrated better performance than Webster's, with a reduction in average delay by 25.6%. In addition, the table highlights the enhanced performance of the DNB controller when it utilizes upstream density in its payoff calculation process compared to utilizing vehicle queues. This indicates that incorporating upstream density data provides more important information to the DNB controller to make better-informed decisions, leading to better traffic management outcomes. Moreover, the DNB controller also contributed to an improved fuel economy, achieving an improvement of up to 7.4% over Webster's fixed-time plan.

Table 4: Performance Statistics for the Isolated Intersection Simulation

TSC	Average Delay (s/veh)	Average FC (liters)
FT-Webster	35.641	0.068
FT-LDR	26.518	0.064
Improvement	*25.6%*	*5.9%*
DNB-Queues	23.480	0.064
Improvement	*34.1%*	*5.9%*
DNB-Density	22.916	0.063
Improvement	*37.7%*	*7.4%*

Distribution of the Cycle Length and phase splits

Figure 18 shows a sample of the switching pattern for each of the three control strategies. This figure illustrates that the DNB controller prioritizes Phases 2 and 4, resulting in more frequent switching compared to the fixed-time plans. This increased flexibility in both the phase switching sequence and the allocated green time for each phase allows the DNB controller to achieve more efficient traffic management.

Figure 18 illustrates the variation in the cycle length produced by the DNB controller, where the cycle length is calculated from the end of the critical phase, which in this case is Phase 4. The figure shows that the cycle length fluctuates between approximately 35 seconds and 75 seconds. These fluctuations indicate that the DNB controller, while not explicitly optimizing the cycle length, generates a dynamically adjusting cycle length to address the demand needs. This adaptability helps in optimizing traffic flow and reducing traffic congestion on the intersection approaches. Furthermore, Figure 20 also displays the distribution of the cycle lengths during the simulation period, where the cycle length around 50 seconds occurs more frequently. This shows the DNB controller's flexibility in adjusting the cycle length dynamically, according to the real-time demand level, further demonstrating its ability to adjust the intersection operation in response to varying traffic conditions.

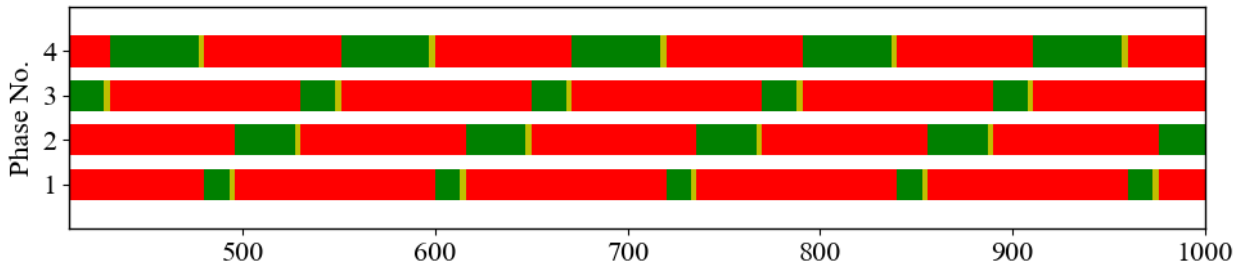

(a)

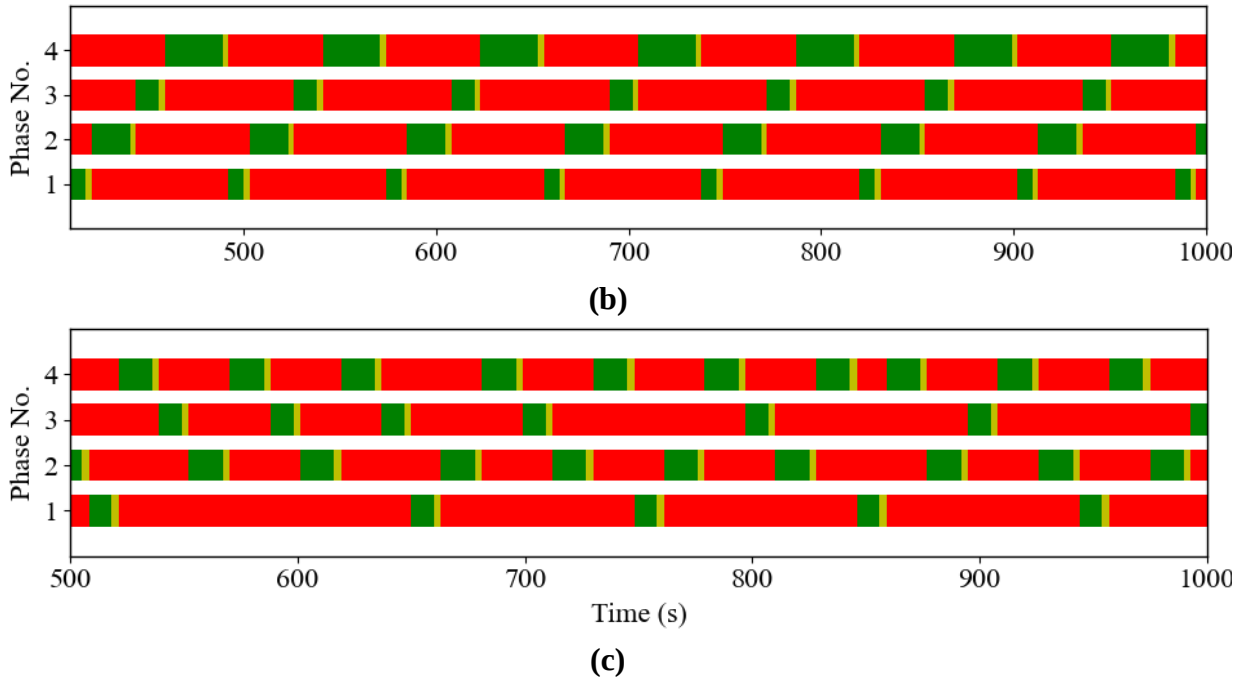

Figure 18: Signal Switching Pattern: (a) Webster Fixed-Time Plan, (b) LDR Fixed-Time Plan, (c) DNB Controller

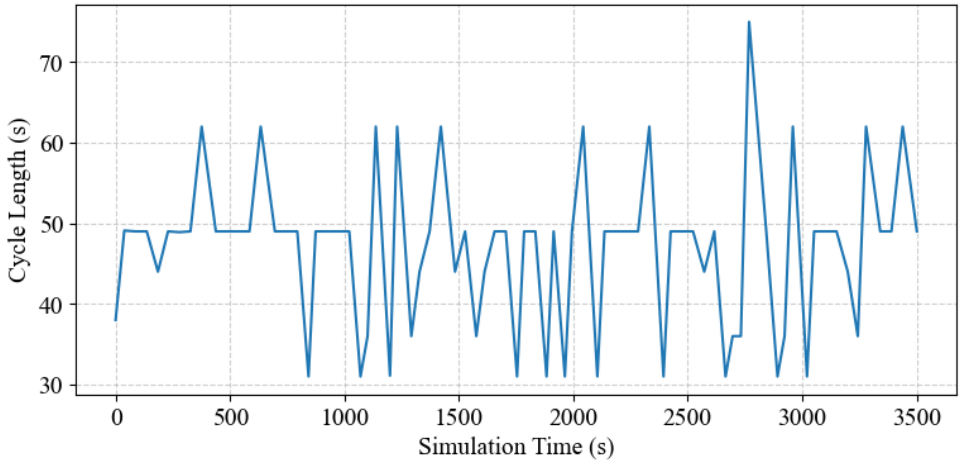

Figure 19: Cycle Length Variation during Simulation

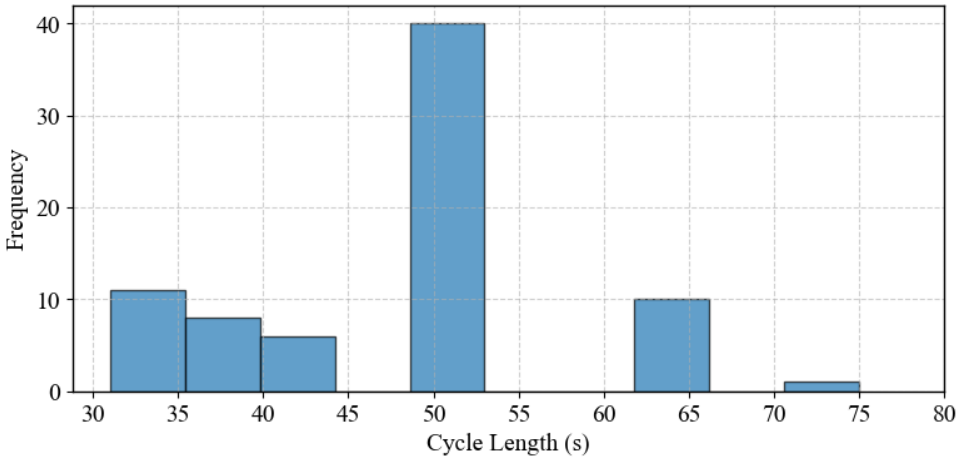

Figure 20: Cycle Length Distribution during Simulation

Results of the Joint DNB-KF Algorithm

Figure 21 presents the average delay across different market penetration levels, benchmarked against the following control strategies:

- **PT-Webster**: A pre-timed signal control strategy with cycle lengths optimized using Webster's method.
- **PT-LDR**: A pre-timed strategy employing the LDR method for cycle length calculation.
- **ACT-Webster**: An actuated signal control strategy with parameters derived from Webster's optimal phase lengths.
- **ACT-LDR**: An actuated strategy using LDR-based optimal phase lengths.
- **DNB (MP=100%)**: The DNB controller's performance under full traffic information availability (100% connected vehicle penetration).

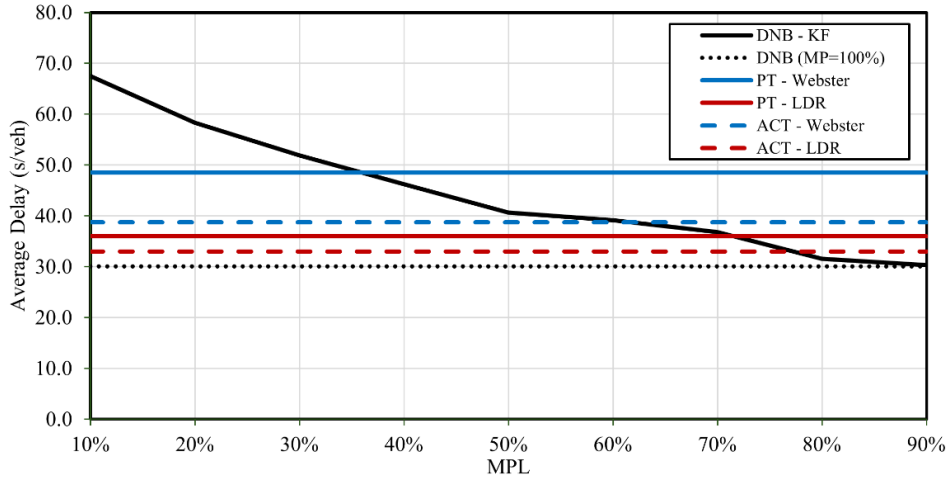

Figure 21: Average delay (s/veh) versus the market penetration level for different Control Strategies at increased demand design by 10% - Toronto Intersection

Discussion

Traffic State Estimation and Prediction

This research highlights the effectiveness of a two-stage approach utilizing Kalman filters for traffic state estimation and prediction, particularly at market penetration levels below 30%. The results demonstrate significant improvements in the accuracy of turning movement, queue size, and density estimations compared to existing methodologies, reaffirming the viability of Kalman filters for real-time applications in traffic management systems. While marginal enhancements were observed at higher penetration levels, the findings underscore the importance of this approach in facilitating adaptive traffic signal controls that require timely and precise data. By addressing common limitations of traditional and machine learning models, our proposed method proves to be a robust solution offering computational efficiency and reliability without reliance on historical traffic data. Looking ahead, the integration of this system with vehicle trajectory optimization and advanced signal control mechanisms presents promising opportunities for improving traffic flow and safety in increasingly congested urban environments. As such, further exploration and practical deployment of the two-stage approach are encouraged to fully realize its potential in transforming modern traffic management.

DNB Results Considering Incomplete Probe Data

The integration of the decentralized Nash-bargaining traffic signal control system with the Kalman filtering traffic state estimation and prediction algorithm presents a significant advancement in traffic management practices. The results from the case studies in Toronto and Orlando highlight the effectiveness of the joint DNB-KF system, demonstrating superior performance over traditional control methods at various market penetration levels. Particularly noteworthy is the system's ability to excel even at lower penetration rates, showcasing its potential to adapt to real-world scenarios with varying traffic conditions and demands. As urban areas continue to grapple

with congestion and mobility challenges, the findings of this research emphasize the critical role that intelligent traffic management systems will play in fostering sustainable urban environments. Future implementation of these advanced methodologies can pave the way for smarter cities, enhancing not only traffic flow but also overall quality of life for residents. It is imperative for urban planners and policymakers to consider these innovative solutions as we move towards a more connected and efficient transportation future.

Summary and Conclusion

This paper presents a two-stage Kalman filter-based approach for real-time traffic state estimation and prediction using probe vehicle and upstream detector data. The first stage estimates turning movements in real time, while the second stage estimates upstream link density and queue lengths at intersections, categorized by movement. To improve the accuracy of Kalman filter inputs, a sampling error analysis is applied to compute the measurement and prediction error covariance matrices using real-time data. The system is evaluated using a drone-collected dataset from a four-legged signalized intersection in Orlando, Florida. Results demonstrate significant improvements in estimation and prediction accuracy, especially at low levels of market penetration. In the first stage, turning movement estimation shows a reduction in error standard deviation by up to 50% compared to methods relying solely on probe vehicle data, with R^2 values improving from –0.14 to 0.70 at 5% market penetration, and reaching 0.94 at 20%. The second stage also demonstrates improved accuracy in queue size and upstream density estimation, with queue MAPE reduced by up to 45% and density estimates improved by up to 18.5%. The proposed method proves effective even at low market penetration rates and offers advantages over machine learning techniques by eliminating the need for historical data and maintaining computational efficiency for real-time use. Its predictive capabilities also make it suitable for integration into vehicle trajectory optimization systems and game-theoretic adaptive traffic signal controllers.

In addition, this study evaluates two alternative isolated traffic signal control strategies aimed at minimizing vehicle delay and emissions. The first strategy applies the Laguna-Du-Rakha (LDR) cycle length optimization method to fixed-time signal planning, while the second involves the enhancement and implementation of a decentralized Nash-bargaining (DNB) traffic signal controller. The DNB controller models traffic signal phases as players in a game-theoretic framework, using queue length and upstream vehicle density as inputs to compute payoff values and determine optimal green indications. A threat point mechanism is also incorporated to prevent spillbacks into upstream intersections or beyond pocket lanes. Both strategies are tested at a high-demand intersection in downtown Toronto, using Poisson arrival processes to reflect real-world variability in traffic flow. The DNB algorithm is further refined to account for inter-green times between phases.

Results show that both the LDR and DNB methods significantly outperform Webster's fixed-time control in terms of reducing queue lengths, vehicle delay, and fuel consumption. Specifically, the LDR method reduces vehicle delay and fuel consumption by 25.6% and 5.9%, respectively. The DNB controller achieves up to a 37.7% reduction in average vehicle delay when using upstream density in its payoff function and a 34.1% reduction when using queue length. It also improves

fuel consumption by 7.4% and 5.9%, respectively, for density- and queue-based calculations. These findings highlight the DNB controller's potential as a dynamic, responsive signal control strategy capable of adapting to real-time traffic conditions.

Finally, this study integrated the Kalman filter algorithm with the DNB algorithm and compared it to the performance of different traffic signal control strategies. These strategies include PT-Webster, a pre-timed controller using Webster’s method for cycle length optimization, and PT-LDR, which applies the LDR method for cycle calculation. The strategies also include two actuated strategies: ACT-Webster, which uses phase lengths based on Webster’s formula, and ACT-LDR, which employs LDR-derived optimal phase lengths. This comparison highlights how average delay evolves with increasing market penetration and underscores the potential benefits of the DNB controller when full real-time traffic data is available.

References

Abdelghaffar, H. M., & Rakha, H. A. (2019). A Novel Decentralized Game-Theoretic Adaptive Traffic Signal Controller: Large-Scale Testing. *Sensors*, *19*(10), 2282. https://doi.org/10.3390/s19102282

Abdelghaffar, H. M., & Rakha, H. A. (2021). Development and Testing of a Novel Game Theoretic De-Centralized Traffic Signal Controller. *IEEE Transactions on Intelligent Transportation Systems*, *22*(1), 231–242. https://doi.org/10.1109/TITS.2019.2955918

Ahmad, F., & Al-Fagih, L. (2024). Travel behaviour and game theory: A review of route choice modeling behaviour. *Journal of Choice Modelling*, *50*, 100472. https://doi.org/10.1016/j.jocm.2024.100472

Ahmad, F., Almarri, O., Shah, Z., & Al-Fagih, L. (2023). Game theory applications in traffic management: A review of authority-based travel modelling. *Travel Behaviour and Society*, *32*, 100585. https://doi.org/10.1016/j.tbs.2023.100585

Aljamal, M. A., Abdelghaffar, H. M., & Rakha, H. A. (2019). Kalman Filter-based Vehicle Count Estimation Approach Using Probe Data: A Multi-lane Road Case Study. *2019 IEEE Intelligent Transportation Systems Conference (ITSC)*, 4374–4379. https://doi.org/10.1109/ITSC.2019.8917360

Alvarez, I., & Poznyak, A. (2010). Game theory applied to urban traffic control problem. *ICCAS 2010*, 2164–2169. https://doi.org/10.1109/ICCAS.2010.5670234

Antoniou, C., Ben-Akiva, M., & Koutsopoulos, H. N. (2007). Nonlinear Kalman Filtering Algorithms for On-Line Calibration of Dynamic Traffic Assignment Models. *IEEE Transactions on Intelligent Transportation Systems*, *8*(4), 661–670. IEEE Transactions on Intelligent Transportation Systems. https://doi.org/10.1109/TITS.2007.908569

Auger, F., Hilairet, M., Guerrero, J. M., Monmasson, E., Orlowska-Kowalska, T., & Katsura, S. (2013). Industrial applications of the kalman filter: A review. *IEEE Transactions on Industrial Electronics*, *60*(12), 5458–5471. https://doi.org/10.1109/TIE.2012.2236994

Bazzan, A. L. C. (2005). A Distributed Approach for Coordination of Traffic Signal Agents. *Autonomous Agents and Multi-Agent Systems*, *10*(2), 131–164. https://doi.org/10.1023/B:AGNT.0000049887.90232.cd

Bekiaris-Liberis, N., Roncoli, C., & Papageorgiou, M. (2016). Highway Traffic State Estimation With Mixed Connected and Conventional Vehicles. *IEEE Transactions on Intelligent Transportation Systems*, *17*(12), 3484–3497. https://doi.org/10.1109/TITS.2016.2552639

Blokpoel, R., & Vreeswijk, J. (2016). Uses of Probe Vehicle Data in Traffic Light Control. *Transportation Research Procedia*, *14*, 4572–4581. https://doi.org/10.1016/j.trpro.2016.05.380

Brown, S. D., & Rutan, S. C. (1985). Adaptive Kalman Filtering. *Journal of Research of the National Bureau of Standards*, *90*(6), 403–407. https://doi.org/10.6028/jres.090.032

Calle-Laguna, A. J., Du, J., & Rakha, H. A. (2019). Computing optimum traffic signal cycle length considering vehicle delay and fuel consumption. *Transportation Research Interdisciplinary Perspectives*, *3*, 100021. https://doi.org/10.1016/j.trip.2019.100021

Cao, J., Hu, D., Hadiuzzaman, Md., Wang, X., & Qiu, T. Z. (2014). Comparison of queue estimation accuracy by shockwave-based and input-output-based models. *17th International IEEE Conference on Intelligent Transportation Systems (ITSC)*, 2687–2692. https://doi.org/10.1109/ITSC.2014.6958120

Chen, A., Chootinan, P., Ryu, S., Lee, M., & Recker, W. (2012). An intersection turning movement estimation procedure based on path flow estimator. *Journal of Advanced Transportation*, *46*(2), 161–176. https://doi.org/10.1002/ATR.151

Chen, X., Zhang, S., Li, L., & Li, L. (2019). Adaptive Rolling Smoothing With Heterogeneous Data for Traffic State Estimation and Prediction. *IEEE Transactions on Intelligent Transportation Systems*, *20*(4), 1247–1258. IEEE Transactions on Intelligent Transportation Systems. https://doi.org/10.1109/TITS.2018.2847024

Comert, G., & Cetin, M. (2011). Analytical Evaluation of the Error in Queue Length Estimation at Traffic Signals From Probe Vehicle Data. *IEEE Transactions on Intelligent Transportation Systems*, *12*(2), 563–573. IEEE Transactions on Intelligent Transportation Systems. https://doi.org/10.1109/TITS.2011.2113375

Elouni, M., Abdelghaffar, H. M., & Rakha, H. A. (2021). Adaptive Traffic Signal Control: Game-Theoretic Decentralized vs. Centralized Perimeter Control. *Sensors*, *21*(1), 274. https://doi.org/10.3390/s21010274

El-Tantawy, S., Abdulhai, B., & Abdelgawad, H. (2014). Design of Reinforcement Learning Parameters for Seamless Application of Adaptive Traffic Signal Control. *Journal of Intelligent Transportation Systems*, *18*(3), 227–245. https://doi.org/10.1080/15472450.2013.810991

Emami, A., Sarvi, M., & Asadi Bagloee, S. (2019). Using Kalman filter algorithm for short-term traffic flow prediction in a connected vehicle environment. *Journal of Modern Transportation*, *27*(3), 222–232. https://doi.org/10.1007/s40534-019-0193-2

Enjedani, S. N., & Khanal, M. (2023). Development of a Turning Movement Estimator Using CV Data. *Future Transportation 2023, Vol. 3, Pages 349-367*, *3*(1), 349–367. https://doi.org/10.3390/FUTURETRANSP3010021

Fadhloun, K., & Rakha, H. (2020). A novel vehicle dynamics and human behavior car-following model: Model development and preliminary testing. *International Journal of Transportation Science and Technology*, *9*(1), Article DOE-VT-0008209-J03. https://doi.org/10.1016/j.ijtst.2019.05.004

Ghanim, M. S., & Shaaban, K. (2019). Estimating Turning Movements at Signalized Intersections Using Artificial Neural Networks. *IEEE Transactions on Intelligent Transportation Systems*, *20*(5), 1828–1836. https://doi.org/10.1109/TITS.2018.2842147

Hao, P., Ban, X. (Jeff), Guo, D., & Ji, Q. (2014). Cycle-by-cycle intersection queue length distribution estimation using sample travel times. *Transportation Research Part B: Methodological*, *68*, 185–204. https://doi.org/10.1016/j.trb.2014.06.004

Hauer, E., Pagitsas, E., & Shin, B. T. (1981). Estimation of Turning Flows from Automatic Counts. *Transportation Research Record*, *795*(001).

Hu, C., Chen, W., Chen, Y., & Liu, D. (2009). Adaptive Kalman Filtering for Vehicle Navigation. *Positioning*, *1*(4), Article 4.

Hu, S., Zhou, Q., Li, J., Wang, Y., Roncoli, C., Zhang, L., & Lehe, L. (2022). High Time-Resolution Queue Profile Estimation at Signalized Intersections Based on Extended Kalman Filtering. *IEEE Transactions on Intelligent Transportation Systems*, *23*(11), 21274–21290. https://doi.org/10.1109/TITS.2022.3173515

Jiao, P., Huapu, L. U., & Yang, L. (2005). Real-time estimation of turning movement proportions based on genetic algorithm. *IEEE Conference on Intelligent Transportation Systems, Proceedings, ITSC*, *2005*, 484–489. https://doi.org/10.1109/ITSC.2005.1520096

Jiao, P., Sun, T., & Du, L. (2014). A Bayesian Combined Model for Time-Dependent Turning Movement Proportions Estimation at Intersections. *Mathematical Problems in Engineering*, *2014*. https://doi.org/10.1155/2014/607195

Kalman, R. E. (1960). A New Approach to Linear Filtering and Prediction Problems. *Journal of Basic Engineering*, *82*(1), 35–45. https://doi.org/10.1115/1.3662552

Karasalo, M., & Hu, X. (2011). An optimization approach to adaptive Kalman filtering. *Automatica*, *47*(8), 1785–1793. https://doi.org/10.1016/j.automatica.2011.04.004

Lan, C. J., & Davis, G. A. (1999). Real-time estimation of turning movement proportions from partial counts on urban networks. *Transportation Research Part C: Emerging Technologies*, *7*(5), 305–327. https://doi.org/10.1016/S0968-090X(99)00025-X

Linglong, T., Xiaohua, Z., Dunli, H., Yanzhang, S., & Ren, W. (2010). A Study of Single Intersection Traffic Signal Control Based on Two-player Cooperation Game Model. *2010 WASE International Conference on Information Engineering*, *2*, 322–327. https://doi.org/10.1109/ICIE.2010.172

Liu, H., Liang, W., Rai, L., Teng, K., & Wang, S. (2019). A Real-Time Queue Length Estimation Method Based on Probe Vehicles in CV Environment. *IEEE Access*, *7*, 20825–20839. IEEE Access. https://doi.org/10.1109/ACCESS.2019.2898424

Mehra, R. (1970). On the identification of variances and adaptive Kalman filtering. *IEEE Transactions on Automatic Control*, *15*(2), 175–184. IEEE Transactions on Automatic Control. https://doi.org/10.1109/TAC.1970.1099422

Mirchandani, P. B., Nobe, S. A., & Wu, W. W. (2001). Online Turning Proportion Estimation in Real-Time Traffic-Adaptive Signal Control. *Transportation Research Record*, *1748*(1), 80–86. https://doi.org/10.3141/1748-10

Mousavizadeh, O., Keyvan-Ekbatani, M., & Logan, T. M. (2021). Real-time turning rate estimation in urban networks using floating car data. *Transportation Research Part C: Emerging Technologies*, *133*, 103457. https://doi.org/10.1016/j.trc.2021.103457

Papageorgiou, M., Diakaki, C., Dinopoulou, V., Kotsialos, A., & Wang, Y. (2003). Review of road traffic control strategies. *Proceedings of the IEEE*, *91*(12), 2043–2067. Proceedings of the IEEE. https://doi.org/10.1109/JPROC.2003.819610

Raghothama, J., & Meijer, S. A. (2014). A Review of Gaming Simulation in Transportation. In S. A. Meijer & R. Smeds (Eds.), *Frontiers in Gaming Simulation* (pp. 237–244). Springer International Publishing. https://doi.org/10.1007/978-3-319-04954-0_28

Rakha, H. A., Ahn, K., Moran, K., Saerens, B., & Bulck, E. V. D. (2011). Virginia Tech Comprehensive Power-Based Fuel Consumption Model: Model development and testing. *Transportation Research Part D: Transport and Environment*, *16*(7), 492–503. https://doi.org/10.1016/j.trd.2011.05.008

Rakha, H., Snare, M., & Dion, F. (2004). Vehicle Dynamics Model for Estimating Maximum Light-Duty Vehicle Acceleration Levels. *Transportation Research Record: Journal of the Transportation Research Board*, *1883*(1), 40–49. https://doi.org/10.3141/1883-05

Rostami-Shahrbabaki, M., Safavi, A. A., Papageorgiou, M., Setoodeh, P., & Papamichail, I. (2020). State estimation in urban traffic networks: A two-layer approach. *Transportation Research Part C: Emerging Technologies*, *115*, 102616. https://doi.org/10.1016/j.trc.2020.102616

Saldivar-Carranza, E. D., Li, H., & Bullock, D. M. (2021). Identifying Vehicle Turning Movements at Intersections from Trajectory Data. *IEEE Conference on Intelligent Transportation Systems, Proceedings, ITSC*, *2021-September*, 4043–4050. https://doi.org/10.1109/ITSC48978.2021.9564781

Schaefer, M. C. (1988). Estimation of Intersection Turning Movements from Approach Counts. *Ite Journal-Institute of Transportation Engineers*.

Srinivasan, D., Choy, M. C., & Cheu, R. L. (2006). Neural Networks for Real-Time Traffic Signal Control. *IEEE Transactions on Intelligent Transportation Systems*, *7*(3), 261–272. https://doi.org/10.1109/TITS.2006.874716

Van Aerde, M., & Rakha, H. (1995). Multivariate calibration of single regime speed-flow-density relationships [road traffic management]. *Pacific Rim TransTech Conference. 1995 Vehicle Navigation and Information Systems Conference Proceedings. 6th International VNIS. A Ride into the Future*, 334–341. https://doi.org/10.1109/VNIS.1995.518858

Van Aerde, M., Rakha, H., & Paramahamsan, H. (2003). Estimation of Origin-Destination Matrices: Relationship Between Practical and Theoretical Considerations. *Transportation Research Record: Journal of the Transportation Research Board*, *1831*(1), 122–130. https://doi.org/10.3141/1831-14

van Lint, H., & Djukic, T. (2012). Applications of Kalman Filtering in Traffic Management and Control. In *New Directions in Informatics, Optimization, Logistics, and Production* (pp. 59–91). INFORMS. https://doi.org/10.1287/educ.1120.0099

Wang, Y., Papageorgiou, M., & Messmer, A. (2008). Real-time freeway traffic state estimation based on extended Kalman filter: Adaptive capabilities and real data testing. *Transportation Research Part A: Policy and Practice*, *42*(10), 1340–1358. https://doi.org/10.1016/j.tra.2008.06.001

Wang, Y., Papageorgiou, M., Messmer, A., Coppola, P., Tzimitsi, A., & Nuzzolo, A. (2009). An adaptive freeway traffic state estimator. *Automatica*, *45*(1), 10–24. https://doi.org/10.1016/j.automatica.2008.05.019

Webster, F. (1958). A Controlled experiment on the capacity of junctions with traffic signals. *Road Research Lab. Res. Note No. RN/3313/FVW. BR, 587*.

Webster, F., & Cobbe, B. (1958). A Controlled experiment on the capacity of junctions with traffic signals. *Road Research Lab. Res. Note No. RN/3313/FVW. BR, 587*.

Wei, L., Li, J., Xu, L., Gao, L., & Yang, J. (2022). Queue Length Estimation for Signalized Intersections under Partially Connected Vehicle Environment. *Journal of Advanced Transportation*, *2022*, 1–11. https://doi.org/10.1155/2022/9568723

Xu, K., Yi, P., Shao, C., Mao, J., Xu, K., Yi, P., Shao, C., & Mao, J. (2013). Development and Testing of an Automatic Turning Movement Identification System at Signalized Intersections. *Journal of Transportation Technologies*, *3*(4), 241–246. https://doi.org/10.4236/JTTS.2013.34025

Zhang, H., Su, Y., Peng, L., & Yao, D. (2010). A review of game theory applications in transportation analysis. *2010 International Conference on Computer and Information Application*, 152–157. https://doi.org/10.1109/ICCIA.2010.6141559

Zhang, X., Cai, X., & Sun, L. (2012). Estimation of Intersection Turning Movement Proportions Using MATLAB. *CICTP 2012: Multimodal Transportation Systems - Convenient, Safe, Cost-Effective, Efficient - Proceedings of the 12th COTA International Conference of Transportation Professionals*, 822–828. https://doi.org/10.1061/9780784412442.084

Zhao, Y., Zheng, J., Wong, W., Wang, X., Meng, Y., & Liu, H. X. (2019). Various methods for queue length and traffic volume estimation using probe vehicle trajectories. *Transportation Research Part C: Emerging Technologies*, *107*, 70–91. https://doi.org/10.1016/j.trc.2019.07.008

Zheng, O., Abdel-Aty, M., Yue, L., Abdelraouf, A., Wang, Z., & Mahmoud, N. (2023). CitySim: A Drone-Based Vehicle Trajectory Dataset for Safety-Oriented Research and Digital Twins. *Transportation Research Record*. https://doi.org/10.1177/03611981231185768